

1 **Reply to Valerie Masson-Delmotte**

2

3 We thank Valerie Masson-Delmotte very much for the comments and final suggestions, which help us
4 further improve the quality of the manuscript. Details on the suggested changes applied on the final
5 version of the manuscript are given below, with page and line numbers corresponding to the manuscript
6 version with marked changes, which is attached to this document after the point-by-point response.

7

8 **Abstract**

9 **P21**

10 **Comment:**

11 Line 9: What is forcing and what is a feedback or a change in the boundary conditions of the climate
12 simulation? I think that the vague use of the word "forcing" is not adequate and should be clarified in
13 the final version.

14 **Reply:**

15 Indeed, all these factors considered in our simulations are not all forcings. The changes in the
16 astronomical parameters represent one forcing, but the changes in GIS and albedo are boundary
17 conditions. Therefore, for clarity, we have replaced “different forcings” with “astronomical forcing and
18 changes in GIS”.

19

20 **Comment:**

21 Line 10: Vague, which season, which amount?

22 **Reply:**

23 We have rephrased the sentence as follows:

24 “The strong Northern Hemisphere summer warming of approximately 2°C (with respect to
25 preindustrial) is mainly caused by increased summer insolation.”.

26

27 **Comment:**

28 Line 13: compared to what

29 **Reply:**

30 We have added: “[...], compared to the purely insolation-driven LIG.”

31

1 **Comment:**
2 Line 14: regional

3 **Reply:**
4 Done.
5

6 **Comment:**
7 Line 19: the magnitude of temperature change when compared to reconstructions

8 **Reply:**
9 We have rephrased as suggested:
10 “Our model results are in good agreement with proxy records with respect to the warming pattern, but
11 underestimate the magnitude of temperature change when compared to reconstructions, [...]”
12

13 **Comment:**
14 Line 21: or missing feedacks (e.g. vegetation)

15 **Reply:**
16 Our model simulations include dynamic vegetation and vegetation feedbacks. Furthermore, we
17 consider that listing potentially relevant missing feedbacks in our model is not necessary in the abstract
18 since it is not the main purpose here, therefore we leave this part related to the model vague, the same
19 as when we mention potential misinterpretation of the proxy record. However, in the Discussion
20 section we do already mention some of these missing feedbacks in our model (Page 43 Line 9).
21

22 **Comment:**
23 Line 29: ice core data

24 **Reply:**
25 Added as suggested.
26

27 **Comment:**
28 Line 28: See also Landais et al?
29 In which season : summer winter?

30 **Reply:**
31 We have added the recommended reference (Landais et al., 2016) in the discussion about model-data

1 comparison in the Discussion section (Page 42 Line 5):

2 “Such dramatic temperature changes at the NEEM site are proposed by another recent study based on
3 ice core air isotopic composition ($\delta^{15}\text{N}$) and relationships between accumulation rate and temperature
4 (Landais et al., 2016). Their study suggests anomalies between the LIG (126 kyr BP) and the PI of +7
5 to +11°C, with +8°C being considered the most likely estimate.”

6

7 Regarding the season, for clarity, we have added in the text “[...] annual mean and summer temperature
8 change [...]”, namely the two temperature averages that we consider in our model-data comparison.

9

10

11

12 **Introduction:**

13 **P22**

14 **Comment:**

15 Line 10: vague : in response to well known changes in astronomical forcing

16 **Reply:**

17 We have rephrased as suggested:

18 “In particular, the simulation of interglacial climates provides an example of how models can respond
19 to well known changes in astronomical forcing [...]”.

20

21 **Comment:**

22 Line 20: in several regions?

23 **Reply:**

24 We have added “in several regions” in the text.

25

26 **Comment:**

27 Line 21: simulated

28 **Reply:**

29 We have added the word “simulated” in the sentence:

30 “Simulated winter in high latitudes is considered to be warmer during the LIG due to sea ice feedbacks
31 [...]”.

1
2
3
4
5
6
7
8
9
10
11
12
13
14
15
16
17
18
19
20
21
22
23
24
25
26
27
28
29
30
31

Comment:

Line 24: Missing reference here (source ice core records or Bakker et al QSR 2015)

Reply:

We have added the Bakker et al. (2014) reference.

P23

Comment:

Line 1: and Masson-Delmotte et al, IPCC, 2013.

Reply:

We have added the Masson-Delmotte et al. (2013) reference.

Comment:

Line 2: there is not single number but a range (6-9 m)

Reply:

We have rephrased as follows:

“An increase in sea level during the LIG is estimated to be between 6 to 9 m [...]”.

Comment:

Line 7: albeit part of the uncertainty arises from different climate scenarios used to assess the ice sheet response.

Reply:

We have rephrased as suggested:

“The contribution of a partially melted GIS to LIG sea level rise is however not yet well determined; various studies suggest a sea level rise due to meltwater from Greenland of +0.3 to +5.5 m (Cuffey and Marshall, 2000; Tarasov and Peltier, 2003; Lhomme et al., 2005; Otto-Bliesner et al., 2006; Colville et al., 2011; Quiquet et al., 2013; Stone et al., 2013), part of the uncertainty arising from different climate scenarios used to assess the ice sheet response.”.

Comment:

1 Line 20: One issue here is that the Greenland ice sheet is expected to thicken at the start of an
2 interglacial period during to enhanced accumulation associated with deglacial warming (see also
3 NEEM 2013).

4 **Reply:**

5 In the latest manuscript version, we have mentioned this issue in the Model-data comparison in the
6 Discussion section, at the part where limitations of our model are discussed (Page 43 Line 12):

7 “For instance, GIS is expected to thicken at the start of an interglacial period due to enhanced
8 accumulation associated with deglacial warming (see also NEEM Community members, 2013).”

9

10

11 **P24**

12 **Comment:**

13 Line 6: have proposed

14 **Reply:**

15 Done.

16

17 **Comment:**

18 Line 18: I think that insolation is a forcing but ice sheet change and albedo change are Earth system
19 feedbacks. Please revisit the wording here.

20 **Reply:**

21 We have rephrased as follows:

22 “Additionally, we assess the importance of insolation and albedo.”

23

24

25

26 **Data & Methods:**

27 **P26**

28 **Comment:**

29 Line 20: remove extra parenthesis

30 **Reply:**

31 Done.

1
2
3
4
5
6
7
8
9
10
11
12
13
14
15
16
17
18
19
20
21
22
23
24
25
26
27
28
29
30
31

P27

Comment:

Line 4: I do not understand this sentence.

You need to explain how you account for the rebound effect in relating changes in surface height to ice volume and sea level contribution.

The statement "instead of 7 m for the present situation" is not clear at all.

Reply:

The lithosphere depression is calculated according to the following equation:

$$x = \frac{h \times \rho_{ice}}{\rho_l - \rho_{ice}},$$

where h is the height of the ice sheet (2600 m for preindustrial GIS and 1300 m for reduced GIS), ρ_{ice} is the density of ice ($\sim 1000 \text{ kg m}^{-3}$), and ρ_l is the density of the lithosphere ($\sim 3300 \text{ kg m}^{-3}$).

However, since this is not the topic of our paper, we did not include the equation in the main manuscript, and only provided a rough estimate of how much the sea level would increase if GIS was reduced to half, not accounting for changes in the lithosphere caused by the ice mass.

With the statement "instead of 7 m for the present situation" we meant that if GIS would completely melt it would contribute 7 m to sea level rise, while half GIS melt would increase the sea level by roughly 3 m. A comma was missing after "7 m".

For clarity, we have rephrased as follows:

"Such changes in GIS elevation and extent would lead to a sea level rise of about 3 m for the present situation, due to the post-glacial rebound effect, when assuming no elastic lithosphere deformation (Fowler, 2004)."

Comment:

Line 10: You should add here : It is however not compatible with the elevation change inferred from the air content at NEEM (NW Greenland) which suggests less than 400 m elevation (albeit with a large uncertainty) decrease starting from an ice sheet thicker than today at the end of the penultimate deglaciation, and along the last interglacial period (NEEM 2013).

Reply:

We have added the suggested sentence.

1
2
3
4
5
6
7
8
9
10
11
12
13
14
15
16
17
18
19
20
21
22
23
24
25
26
27
28
29
30
31

Comment:

Line 29: greenhouse

Reply:

We have replaced the word “trace” with the word “greenhouse”.

P28

Comment:

Line 21: (missing reference here, e.g. Loutre or Braconnot)

Reply:

We have added the following references: Joussaume and Braconnot (1997) and Lorenz and Lohmann (2004).

P29

Comment:

Line 13: please reformulate "plateaued".

Reply:

We have replaced the word “plateaued” with “leveled”.

Results:

P30

Comment:

Line 5: replace "global TS" by : "presents the global effect on TS of ..."

Reply:

We have rephrased as follows:

“Figure 2 shows the TS changes of lowering GIS by various methods.”

1 **Comment:**

2 Line 10: I do not understand what you mean by "global mean (southern hemisphere)". Please change to
3 hemispheric mean if this is the right term.

4 **Reply:**

5 We have rephrased as follows:

6 “Considering all LIG sensitivity simulations, the highest TS mean anomalies globally and in the
7 Southern Hemisphere are simulated in LIG-1300m-alb, with an average of $\Delta TS = +0.37^{\circ}\text{C}$ and $\Delta TS =$
8 $+0.31^{\circ}\text{C}$, respectively (Table 2).”.

9

10 **Comment:**

11 Line 18: is this hemispheric or global? Please clarify.

12 **Reply:**

13 Here, it refers to the northern high latitudes. For clarity, we have rephrased as follows:

14 “This indicates that albedo plays a significant role in the temperature changes over northern high
15 latitudes, where it is causing an average temperature anomaly of $\Delta TS = +0.42^{\circ}\text{C}$.”.

16

17 **Comment:**

18 Line 25: This is very hard to read as you use different references. I suggest to say that it leads to a
19 smaller reduction of AMOC (3.5-2.2=1.3 Sv) relative to the PI.

20 => Can you explain the mechanism at play?

21 => Can you assess the significance of the change?

22 **Reply:**

23 We have rephrased as suggested:

24 “At 130 kyr BP, the AMOC was reduced by 3.5 Sv as compared to the PI (Table 2). However, a
25 reduction in GIS partly counteracts the negative anomaly and leads to a smaller reduction of AMOC
26 (3.5-2.2=1.3 Sv) relative to the PI (Table 2).”.

27

28 The potential explanation of the mechanism is already described in the Discussion section (Page 38
29 Line 11).

30

31 We have performed an independent two-tailed Student's *t*-test *t* and found that the changes in AMOC

1 between the LIG-ctl and PI, and LIG-1300m-alb and LIG-ctl, and LIG-1300m-alb and PI are all
2 statistically significant. We have added this information in the paragraph:
3 “After performing an independent two-tailed Student's t test t with 95% confidence interval, we find
4 that these changes in AMOC are statistically significant.”

5
6

7 **P32**

8 **Comment:**

9 Line 6: You may want to argue whether this is related to enhanced summer monsoons and associated
10 surface cooling as reported in earlier studies.

11 **Reply:**

12 An explanation related to the cooling in these regions is already given in the Discussion section (Page
13 37 Line 15).

14

15 **Comment:**

16 Line 10: replace "in dependence of the location" by : " as a function of the location as well as season".

17 **Reply:**

18 Done as suggested.

19

20

21 **P33**

22 **Comment:**

23 Line 23: Here please be very cautious in reporting the comparison between the Greenland ice core data
24 and the simulation.

25 Please carefully check whether the reconstructions account or not for changes in local elevation
26 (temperature "at fixed elevation" or not).

27 The only record spanning the LIG is from NEEM ice core and a new reconstruction is currently
28 submitted by Landais et al (Clim Past Discussion).

29 **Reply:**

30 The two ice core records (NGRIP and Renland) from the CAPE Last Interglacial Project Members
31 (2006) included in our model-data comparison do not seem to account for changes in local elevation.

1 We have included in the Discussion also the reconstruction from Landais et al. (2016) (Page 42 Line 5).

2

3

4 **P34**

5 **Comment:**

6 Line 8: what do you mean by "annual mean minimum or maximum LIG warmth"? I do not understand
7 this sentence.

8 **Reply:**

9 Annual mean minimum LIG warmth represents the coldest 100 model years, while annual mean
10 maximum LIG warmth represents the warmest 100 model years of the respective transient simulation.
11 A definition of these averages is already included in Data and Methods section (Page 28 Line 24).

12 “Maximum and minimum LIG TS are calculated from the transient simulations considering the time
13 interval between 130 and 120 kyr BP. In order to filter out internal variability, a 100-point running
14 average representing the average over 1000 calendar years is applied. Maximum and minimum LIG
15 warmth of the summer are defined as the warmest and coldest average of 100 warmest months,
16 respectively, which reflects the warmest or coldest 1000 summer seasons with respect to the
17 astronomical forcing. For the maximum and minimum LIG warmth of annual mean, we consider the
18 warmest and coldest average of 100 model years, respectively. The seasonality range is defined by
19 calculating the summer maximum LIG warmth (warmest average of 100 warmest months of the model
20 years) and winter minimum LIG TS (coldest average of 100 coldest months of the model years).”

21

22 **Comment:**

23 Line 10: This conclusion lies on the hypothesis that the model is realistic.

24 **Reply:**

25 We have added: “[...], when assuming that the model is realistic”.

26

27

28 **P35**

29 **Comment:**

30 Line 3: the amplitude of the signal depicted by reconstructions.

31 (the sentence "model still underestimates the proxy reconstruction" is awkward).

1 **Reply:**

2 We have rephrased as suggested.

3

4 **Comment:**

5 Line 15: simulated

6 **Reply:**

7 Done.

8

9

10 **P36**

11 **Comment:**

12 Line 17: Can this be linked to the fact that the model shows very little AMOC change in the simulation
13 with the GIS reduction compared to the PI simulation?

14 **Reply:**

15 We think that the North Atlantic Ocean presents only a modest change in TS because of a missing
16 factor in our simulations, namely the meltwater input from the remnant Northern Hemisphere ice sheets
17 into the North Atlantic Ocean. We have added the following sentence in the main text:

18 “The melting of the remnant Northern Hemisphere ice-sheets from the penultimate glaciation leads to a
19 cooling of the North Atlantic Ocean (Stone et al., 2016), a factor that is not considered in our
20 simulations, which indicate only a modest change in this region.”.

21

22 **Comment:**

23 Line 22: the model underestimates the amplitude of the signal when compared to reconstructions.

24 **Reply:**

25 We have rephrased as suggested.

26

27

28 **P37**

29 **Comment:**

30 Line 4: of the signal depicted by the proxy records in our simulation is again identified,

31 **Reply:**

1 We have rephrased as suggested.

2

3 **Comment:**

4 Line 4: overestimation of what?

5 **Reply:**

6 overestimation of the signal depicted by the proxy records. For clarity, we have rephrased as follows:

7 “Depending on the location, an underestimation or overestimation of the signal depicted by the proxy
8 records in our simulation is again identified (Figs. S13 and S14).”.

9

10

11

12 **Discussion:**

13 **Comment:**

14 Line 19: but is there any effect of the GIS on this monsoon cooling signal?

15 **Reply:**

16 The cooling observed around 10°N over Africa and 25°N over Arabian Peninsula and India is caused
17 by insolation changes between the LIG and the PI. GIS has little to no influence on the low latitudes (as
18 shown in Fig. 2a,b,c).

19

20 **Comment:**

21 Line 27: This was quantified in Masson-Delmotte Clim Past 2011 ("Sensitivity of Greenland...") with a
22 focus on the insolation driven feedbacks (sea ice, water vapour, clouds etc).

23 **Reply:**

24 We have added the following sentence:

25 “A systematic analysis of insolation-driven feedbacks (e.g. sea ice, water vapors, clouds) has been done
26 by Masson Delmotte et al. (2011)”.

27

28

29 **P38**

30 **Comment:**

31 Line 3: also leads

1 **Reply:**

2 Done.

3

4 **Comment:**

5 Line 30: replace "relative" by "in response to"

6 **Reply:**

7 Done.

8

9

10 **P39**

11 **Comment:**

12 Line 6: maybe stress that this was done with a simplified atmosphere in an EMIC?

13 **Reply:**

14 We have rephrased as follows:

15 “In the study by Bakker et al. (2012) using a simplified atmosphere model, reducing GIS elevation and
16 extent leads to changes in the atmospheric flow pattern and creates a special pattern of surface pressure
17 anomalies.”.

18

19 **Comment:**

20 Line 8: ,

21 **Reply:**

22 Done.

23

24

25 **P41**

26 **Comment:**

27 Line 1: Could you explain this?

28 Is this related to the interplay with orbital forcing?

29 **Reply:**

30 It is not clear why GIS has a stronger influence at the beginning of the LIG than at the late LIG. We
31 gave as a possible explanation the one suggested above, and therefore added:

1 “In our LIG transient simulations, we find that the differences in TS between the different model
2 simulations at the beginning of the LIG (130 kyr BP) are higher than during the late LIG (115 kyr BP),
3 indicating that the impact of a reduced GIS is stronger at the beginning of the LIG as compared to
4 glacial inception (GI, 115 kyr BP), possibly related to an interplay with insolation forcing.”

5

6 **Comment:**

7 Line 21: where their simulation...

8 **Reply:**

9 Done as suggested.

10

11 **Comment:**

12 Line 25: Again the model does not overestimate the reconstructed temperature, but the amplitude of
13 temperature change when compared to reconstructions. Please check rigorously the manuscript to avoid
14 awkward phrasing.

15 **Reply:**

16 We have rephrased as suggested:

17 “A high overestimation of the amplitude of the temperature change by the model is found also by [...]”.

18 Furthermore, we have correctly rephrased all such sentences throughout the manuscript.

19

20 **Comment:**

21 Line 30: Attention : this estimate is "at fixed elevation" (after correction for the elevation change).

22 Can you please make sure that the comparison is achieved in a coherent framework?

23 -> model with change in elevation with NEEM without elevation correction, for instance?

24 You can also refer to Landais et al Clim Past Discussions 2016 that include other sources of
25 information (air isotopes) and confirm the amplitude of warming.

26 **Reply:**

27 For consistency, we have also included the temperature estimate before the correction for the elevation
28 changes, and we added:

29 Page 42 Line 4: “When the temperature estimate from NEEM ice core is not corrected for elevation
30 changes, it indicates a positive anomaly of $7.5 \pm 1.8^\circ\text{C}$.”.

31

1 We have also added the suggested reference:

2 Page 42 Line 5: “Such dramatic temperature changes at the NEEM site are proposed by another recent
3 study based on ice core air isotopic composition ($\delta^{15}\text{N}$) and relationships between accumulation rate
4 and temperature (Landais et al., 2016). Their study suggests anomalies between the LIG (126 kyr BP)
5 and the PI of +7 to +11°C, with +8°C being considered the most likely estimate.”

6
7

8 **P42**

9 **Comment:**

10 Line 11: Moreover, our study does not account for possible changes in the Antarctic ice sheet
11 topography and its potential impacts

12 (here there is a recent study for which Eric Steig is a co author and may be cited).

13 **Reply:**

14 We have added the sentence as suggested and referred to the work done recently here at AWI by Sutter
15 et al. (2016). In that publication, all the relevant references can be found.

16 “Moreover, our study does not account for possible changes in the Antarctic ice sheet topography and
17 its potential impacts (Sutter et al., 2016 and references therein).”

18
19

20 **P43**

21 **Comment:**

22 Line 9: This sentence is very difficult to read. I suggest :

23 This also calls to perform LIG simulations in Earth system models that account for feedbacks not
24 accounting for in our simulations, such as those associated with soils (REF) and fully interactive ice
25 sheets (REF).

26 **Reply:**

27 Rephrased as follows:.

28 “This also calls to perform LIG simulations in Earth system models that account for feedbacks not
29 accounted for in our simulations, such as those associated with interactive soils (Stärz et al., 2016) and
30 interactive ice sheet model components (Barbi et al., 2014; Gierz et al., 2015).”

31

1 **Comment:**

2 Line 26: I suggest to reformulate to :

3 Otto-Bliesner et al (2013) suggested that this mismatch may arise from the lack of vegetation feedback.

4 Here, the fact that we account for the vegetation feedback challenges this explanation.

5 **Reply:**

6 Rephrased as suggested.

7

8 **Comment:**

9 Line 31: No the model undestimates the amplitude of changes when compared to reconstructions

10 **Reply:**

11 Rephrased as suggested.

12

13

14 **P44**

15 **Comment:**

16 Line 1: has too large simulated changes when compared to the same reconstruction

17 **Reply:**

18 Rephrased as suggested.

19

20 **Comment:**

21 Line 14: You may want to discuss whether your model simulates a larger or weaker change in sea ice
22 compared with the other simulations.

23 **Reply:**

24 Our model simulates a reduction in sea ice in the simulations with reduced GIS compared to the PI. We
25 have added the following sentence:

26 “Along with the simulated increase in TS, there is an annual mean reduction in sea ice in the
27 simulations with reduced GIS compared to the PI (not shown).”

28

29 **Comment:**

30 Line 17: Capron et al (2014) had compared their data compilation to two other climate model
31 simulations, namely...

1 **Reply:**

2 Rephrased as suggested.

3

4 **Comment:**

5 Line 26: This is speculative : can you quantify if the vegetation feedback is that important?

6 **Reply:**

7 We concluded that the vegetation feedback can lead to a cooling after comparing the simulation with
8 fixed preindustrial vegetation (LIG-GHG-tr) with the simulation with dynamic vegetation (LIG-ctl-tr).
9 The only other difference between these two simulations are the GHG concentrations. In the one with
10 dynamic vegetation (LIG-ctl-tr), the CO₂ is fixed to 278 ppmv, while the simulation with fixed
11 preindustrial vegetation (LIG-GHG-tr) has transient CO₂ concentrations, which are mostly lower than
12 278 ppmv, with differences of up to 21 ppmv at 130 kyr BP and up to 15 ppmv later in the simulation.
13 And although one would expect the simulation with higher GHG concentrations (LIG-ctl-tr) to show
14 higher temperatures, we find that actually the simulation with lower GHGs (LIG-GHG-tr) indicates
15 larger temperatures. Thus, one probable cause for this cooling in the simulation with higher CO₂
16 concentration (LIG-ctl-tr) is the vegetation.

17 As for quantifying the importance of the vegetation feedback, we can at least say that a CO₂
18 concentration difference of 15 ppmv is not enough to counteract the cooling caused by vegetation. At
19 the beginning of the simulations, the LIG-ctl-tr has a CO₂ concentration of 21 ppmv more than the
20 LIG-GHG-tr, and indicates indeed higher temperatures. But after that, the role changes for the rest of
21 the simulations. We added in the text:

22 “The vegetation feedback counteracts the warming caused by predominantly higher GHG
23 concentrations; throughout the simulation with dynamic vegetation (LIG-ctl-tr), the CO₂ concentration
24 is higher with up to 15 ppmv than in the simulation with fixed preindustrial vegetation (LIG-GHG-tr).
25 However, higher temperatures are found for the simulation with lower GHG concentrations (LIG-
26 GHG-tr).”.

27

28

29 **P45**

30 **Comment:**

31 Line 21: and further applied in Govin et al (2015).

1 **Reply:**

2 Done.

3

4

5

6 **References in this response:**

7

- Bakker, P., Van Meerbeeck, C. J., and Renssen, H.: Sensitivity of the North Atlantic climate to Greenland Ice Sheet melting during the Last Interglacial, *Clim. Past*, 8, 995–1009, doi:10.5194/cp-8-995-2012, 2012.
- Bakker, P., Masson-Delmotte, V., Martrat, B., Charbit, S., Renssen, H., Gröger, M., Krebs-Kanzow, U., Lohman, G., Lunt, D. J., Pfeiffer, M., Phipps, S. J., Prange, M., Ritz, S. P., Schulz, M., Stenni, B., Stone, E. J., and Varma, V.: Temperature trends during the Present and Last Interglacial periods – a multi-model–data comparison, *Quaternary Sci. Rev.*, 99, 224–243, doi:10.1016/j.quascirev.2014.06.031, 2014.
- Barbi, D., Lohmann, G., Grosfeld, K., and Thoma, M.: Ice sheet dynamics within an Earth system model: coupling and first results on ice stability and ocean circulation, *Geosci. Model Dev.*, 7, 2003–2013, doi:10.5194/gmd-7-2003-2014, 2014.
- CAPE-members – Anderson, P., Bennike, O., Bigelow, N., Brigham-Grette, J., Duvall, M., Edwards, M., Fréchette, B., Funder, S., Johnsen, S., Knies, J., Koerner, R., Lozhkin, A., MacDonald, G., Marshall, S., Matthiessen, J., Miller, G., Montoya, M., Muhs, D., Otto-Bliesner, B., Overpeck, J., Reeh, N., Sejrup, H. P., Turner, C., and Velichko, A.: Last Interglacial Arctic warmth confirms polar amplification of climate change, *Quaternary Sci. Rev.*, 25, 1383–1400, doi:10.1016/j.quascirev.2006.01.033, 2006.
- Capron, E., Govin, A., Stone, E. J., Masson-Delmotte, V., Mulitza, S., Otto-Bliesner, B. L., Rasmussen, T. L., Sime, L. C., Waelbroeck, C., and Wolff, E. W.: Temporal and spatial structure of multi-millennial temperature changes at high latitudes during the Last Interglacial, *Quaternary Sci. Rev.*, 103, 116–133, doi:10.1016/j.quascirev.2014.08.018, 2014.
- Colville, E. J., Carlson, A. E., Beard, B. L., Hatfield, R. G., Stoner, J. S., Reyes, A. V., and Ullman, D. J.: Sr-Nd-Pb isotope evidence for ice-sheet presence on southern Greenland during the last interglacial, *Science*, 333 (6042), 620–623, doi:10.1126/science.1204673, 2011.
- Cuffey, K. M. and Marshall, S. J.: Substantial contribution to sea-level rise during the last interglacial from the Greenland ice sheet, *Nature*, 404, 591–594, doi:10.1038/35007053, 2000.
- Fowler, C. M. R.: *The Solid Earth: an introduction to global geophysics*, Cambridge University Press, doi:10.1017/CBO9780511819643, 2004.
- Gierz, P., Lohmann, G., and Wei, W.: Response of Atlantic Overturning to Future Warming in a coupled Atmosphere-Ocean-Ice Sheet Model, *Geophys. Res. Lett.*, 42, 6811–6818, doi:10.1002/2015GL065276, 2015.

- Govin, A., Capron, E., Tzedakis, P. C., Verheyden, S., Ghaleb, B., Hillaire-Marcel, C., St-Onge, G., Stoner, J. S., Bassinot, F., Bazin, L., Blunier, T., Combourieu Nebout, N., El Quahabi, A., Genty, D., Gersonde, R., Jiminez-Amat, P., Landais, A., Martrat, B., Masson-Delmotte, V., Parrenin, F., Seidenkrantz, M. S., Veres, D., Waelbroeck, C., and Zahn, R.: Sequence of events from the onset to the demise of the Last Interglacial: evaluating strengths and limitations of chronologies used in climatic archives, *Quaternary Sci. Rev.*, 129, 1–36, doi:10.1016/j.quascirev.2015.09.018, 2015.
- Joussaume, S. and Braconnot, P.: Sensitivity of paleoclimate simulation results to season definitions, *J. Geophys. Res.*, 102, 1943–1956, doi:10.1029/96JD01989, 1997.
- Landais, A., Masson-Delmotte, V., Capron, E., Langebroek, P. M., Bakker, P., Stone, E. J., Merz, N., Raible, C. C., Fischer, H., Orsi, A., Prié, F., Vinther, B., and Dahl-Jensen, D.: How warm was Greenland during the last interglacial period?, *Clim. Past Discuss.*, doi:10.5194/cp-2016-28, in review, 2016.
- Lhomme, N., Clarke, G. K. C., and Ritz, C.: (2005): Global budget of water isotopes inferred from polar ice sheets, *Geophys. Res. Lett.*, 32, L20502, doi:10.1029/2005GL023774, 2005.
- Lorenz, S. J. and Lohmann, G.: Acceleration technique for Milankovitch type forcing in a coupled atmosphere–ocean circulation model: method and application for the Holocene, *Clim. Dynam.*, 23, 727–743, doi:10.1007/s00382-004-0469-y, 2004.
- Masson-Delmotte, V., Braconnot, P., Hoffmann, G., Jouzel, J., Kageyama, M., Landais, A., Lejeune, Q., Risi, C., Sime, L., Sjolte, J., Swingedouw, D., and Vinther, B.: Sensitivity of interglacial Greenland temperature and $\delta^{18}\text{O}$: ice core data, orbital and increased CO_2 climate simulations, *Clim. Past*, 7, 1041–1059, doi:10.5194/cp-7-1041-2011, 2011.
- Masson-Delmotte, V., Schulz, M., Abe-Ouchi, A., Beer, J., Ganopolski, A., González Rouco, J. F., Jansen, E., Lambeck, K., Luterbacher, J., Naish, T., Osborn, T., Otto-Bliesner, B., Quinn, T., Ramesh, R., Rojas, M., Shao, X., and Timmermann, A.: Information from Paleoclimate archives, in: *Climate Change 2013: The Physical Science Basis, Contribution of Working Group I to the Fifth Assessment Report of the Intergovernmental Panel on Climate Change*, edited by: Stocker, T. F., Qin, D., Plattner, G.-K., Tignor, M., Allen, S. K., Boschung, J., Nauels, A., Xia, Y., Bex, V., and Midgley, P. M., Cambridge University Press, Cambridge, UK and New York, USA, 383–464, 2013.
- NEEM community members: Eemian interglacial reconstructed from a Greenland folded ice core, *Nature*, 493, 498–494, doi:10.1038/nature11789, 2013.
- Otto-Bliesner, B. L., Marshall, S. J., Overpeck, J. T., Miller, G. H., Hu, A., and CAPE Last Interglacial Project members: simulating Arctic Climate Warmth and Icefield Retreat in the Last Interglaciation, *Science*, 311, 1751–1753, doi:10.1126/science.1120808, 2006.
- Otto-Bliesner, B. L., Rosenbloom, N., Stone, E. J., McKay, N. P., Lunt, D. J., Brady, E. C., and Overpeck, J. T.: How warm was the last interglacial? New model – data comparisons, *Philos. T. R. Soc. A*, 371, 1–20, doi:10.1098/rsta.2013.0097, 2013.
- Quiquet, A., Ritz, C., Punge, H. J., and Salas y Méliá, D.: Greenland ice sheet contribution to sea level rise during the last interglacial period: a modelling study driven and constrained by ice core data, *Clim. Past*, 9, 353–366, doi:10.5194/cp-9-353-2013, 2013.

- Stärz, M., Lohmann, G., and Knorr, G.: The effect of a dynamic soil scheme on the climate of the mid-Holocene and the Last Glacial Maximum, *Clim. Past*, 12, 151–170, doi:10.5194/cp-12-151-2016, 2016.
- Stone, E. J., Lunt, D. J., Annan, J. D., and Hargreaves, J. C.: Quantification of the Greenland ice sheet contribution to Last Interglacial sea level rise, *Clim. Past*, 9, 621–639, doi:10.5194/cp-9-621-2013, 2013.
- Stone, E. J., Capron, E., Lunt, D. J., Payne, A. J., Singarayer, J. S., Valdes, P. J., and Wolff, E. W.: Impact of melt water on high latitude early Last Interglacial climate, *Clim. Past Discuss.*, doi:10.5194/cp-2016-11, in review, 2016.
- Tarasov, L. and W. R. Peltier: Greenland glacial history, borehole constraints, and Eemian extent, *J. Geophys. Res.*, 108(B3), 2143, doi:10.1029/2001JB001731, 2003.

1 Abstract

2 During the Last Interglacial (LIG, ~130–115 kiloyear (kyr) before present (BP)), the northern high
3 latitudes were characterized by higher temperatures than those of the late Holocene and a lower
4 Greenland Ice Sheet (GIS). However, the impact of a reduced GIS on the global climate has not yet
5 been well constrained. In this study, we quantify the contribution of the GIS to LIG warmth by
6 performing various sensitivity studies based on equilibrium simulations, employing the Community
7 Earth System Models (COSMOS), with a focus on height and extent of the GIS. We present the first
8 study on the effects of a reduction in GIS on the surface temperature (TS) on a global scale and
9 separate the contribution of ~~different astronomical~~ forcings and changes in GIS to LIG warmth. The
10 strong Northern Hemisphere summer warming of approximately 2°C (with respect to preindustrial) is
11 mainly caused by increased summer insolation. Reducing the height by ~1300 m and the extent of the
12 GIS does not have a strong influence during summer, leading to an additional global warming of only
13 +0.24°C, compared to the purely insolation-driven LIG. The effect of a reduction in GIS is however
14 strongest during local winter, with up to +5°C regional warming and with an increase in global average
15 temperature of +0.48°C.

16 In order to evaluate the performance of our LIG simulations, we additionally compare the simulated
17 TS anomalies with marine and terrestrial proxy-based LIG temperature anomalies derived from three
18 different proxy data compilations. Our model results are in good agreement with proxy records with
19 respect to the warming pattern, but underestimate the magnitude of temperature change when compared
20 to reconstructionsthe reconstructed temperatures, suggesting a potential misinterpretation of the proxy
21 records or deficits ~~of~~ in our model. However, we are able to partly reduce the mismatch between model
22 and data by additionally taking into account the potential seasonal bias of the proxy record and/or the
23 uncertainties in the dating of the proxy records for the LIG thermal maximum. The seasonal bias and
24 the uncertainty of the timing are estimated from new transient model simulations covering the whole
25 LIG. The model-data comparison improves for proxies that represent annual mean temperatures when
26 GIS is reduced and when we take the local thermal maximum during the LIG (130-120 kyr BP) into
27 account. For proxy data that represent summer temperatures, changes in GIS are of minor importance
28 for sea surface temperatures. However, the annual mean and summer temperature change over
29 Greenland in the reduced GIS simulations seems to be overestimated as compared to the local ice core
30 data, which could be related to the interpretation of the recorder system and/or the assumptions of GIS
31 reduction. Thus, the question regarding the real size of the GIS during the LIG has yet to be answered.

1 **1. Introduction**

2 One important application of atmosphere–ocean general circulation models (AOGCMs) is the
3 computation of future climate projections (Collins et al., 2013; Kirtman et al., 2013), which allow
4 insight into possible future climate states that may be notably different from present day. In order to
5 ensure the reliability of such climate projections, the climate models’ ability to replicate climate states
6 that are different from the present needs to be tested (e.g. Braconnot et al., 2012; Flato et al., 2013).
7 Past time periods provide the means for evaluating the performance of general circulation models (e.g.
8 Dowsett et al., 2013; Lohmann et al., 2013; Lunt et al., 2013).

9 In particular, the simulation of interglacial climates provides an example of how models can
10 respond ~~to well known changes in astronomical forcing when strong changes in the forcing are applied~~
11 (Mearns et al., 2001) and the possibility to analyze the main drivers leading to an interglacial climate
12 that was warmer than the present interglacial. The Last Interglacial (LIG, ~130–115 kiloyear (kyr)
13 before present (BP)) is considered to be on average warmer than the Holocene (10–0 kyr BP)
14 (CLIMAP Project Members, 1984; Martinson et al., 1987; Kukla et al., 2002; Bauch and Erlenkeuser,
15 2003; Felis et al., 2004; Kaspar et al., 2005; Jansen et al., 2007; Turney and Jones, 2010; Masson-
16 Delmotte et al., 2013). Model simulations indicate a pronounced warming during boreal summer in
17 northern high latitudes (Harrison et al., 1995; Kaspar et al., 2005; Otto-Bliesner et al., 2006; Lohmann
18 and Lorenz, 2007; Stone et al., 2013). Proxy records located in the Northern Hemisphere indicate also
19 that LIG climate is characterized by temperatures that are several degrees Celsius above preindustrial
20 values in several regions (Kaspar et al., 2005; CAPE Last Interglacial Project Members, 2006; Turney
21 and Jones, 2010; McKay et al., 2011). Simulated ~~W~~winter in high latitudes is considered to be warmer
22 during the LIG due to sea ice feedbacks (Montoya et al., 2000; Kaspar et al., 2005; Yin and Berger,
23 2010). One cause for LIG summer warmth was increased summer insolation at middle to high latitudes.
24 Greenhouse gas (GHG) concentrations during the LIG were similar to the preindustrial (PI) (Bakker et
25 al., 2014).

26 Studies based on reconstructions and climate model simulations suggest a partial or complete
27 absence of the Greenland Ice Sheet (GIS) during the LIG, and that the sea level was higher than the PI
28 (Veeh, 1966; Stirling et al., 1998; Cuffey and Marshall, 2000; Otto-Bliesner et al., 2006; Overpeck et
29 al., 2006; Jansen et al., 2007; Kopp et al., 2009, 2013; Alley et al., 2010; van de Berg et al., 2011;
30 Robinson et al., 2011; Dutton and Lambeck, 2012; Quiquet et al., 2013; Church et al., 2013; Stone et
31 al., 2013), while a more recent study based on ice core data proposes only a modest GIS change (i.e.

1 equivalent to a contribution to sea level rise of ~2 m, NEEM Community members, 2013; Masson-
2 Delmotte et al., 2013). An increase in sea level during the LIG is estimated to be between of about 6 to
3 97 m (Kopp et al., 2009; Dutton et al., 2015), with a possible contribution of 3 to 4 m from Antarctica
4 (Sutter et al., 2015). The contribution of a partially melted GIS to LIG sea level rise is however not
5 yet well determined; various studies suggest a sea level rise due to meltwater from Greenland of +0.3 to
6 +5.5 m (Cuffey and Marshall, 2000; Tarasov and Peltier, 2003; Lhomme et al., 2005; Otto-Bliesner et
7 al., 2006; Colville et al., 2011; Quiquet et al., 2013; Stone et al., 2013). part of the uncertainty arising
8 from different climate scenarios used to assess the ice sheet response.

9 Existing studies on the effects of a reduced GIS during the LIG have been centered mostly on the
10 Northern Hemisphere and focused on implications related to sea level rise (Stone et al., 2013) and
11 Atlantic Meridional Overturning Circulation (AMOC) (Bakker et al., 2012). The studies by Bakker et
12 al. (2012) and Stone et al. (2013) assume a relatively modest reduction of the GIS and find a mismatch
13 between the simulated and the proxy-based temperature anomalies with respect to PI (CAPE Last
14 Interglacial Project Members, 2006). Otto-Bliesner et al. (2006) find that a GIS elevation reduced by
15 500 m leads to a pronounced warming of up to +5°C in middle to high latitude summer. However, they
16 find as well a mismatch between model and data, with the model underestimating the temperature
17 anomaly indicated by the proxy record. In an LIG study based on transient climate model simulations
18 performed with an earth system model of intermediate complexity (EMIC), Loutre et al. (2014) find
19 that changes in the Northern Hemisphere ice sheets configuration (extent and albedo) have only a small
20 impact on the climate at the beginning of the LIG. They find as well an that the model
21 underestimates the magnitude of the reconstructed temperature change when compared to
22 reconstructions by the models.

23 Other model-data comparison studies for the LIG (Lunt et al., 2013; Otto-Bliesner et al., 2013),
24 based on AOGCMs (but with no changes in GIS elevation or extent) also show an underestimation of
25 temperature global reconstructions temperature anomalies (Turney and Jones, 2010; McKay et al.,
26 2011). Bakker and Renssen (2014), who perform an analysis of transient simulations for the LIG,
27 provide a partial explanation for the model-data mismatch, proposing that such large differences
28 between the reconstructed and simulated LIG temperatures may stem from the fact that commonly-
29 used climate syntheses represent a single time-slice assuming synchronous LIG thermal maximum in
30 space and time. Their study suggests that global compilations of reconstructed LIG thermal maximum
31 overestimate the warming. However, different studies (modelling as well as proxy-based) indicate that

1 the maximum LIG warmth occurred at different times throughout the LIG in dependence of the
2 geographical location (Bakker et al., 2012; Govin et al., 2012; Langebroek and Nisancioglu, 2014). The
3 lack of climate synthesis for the LIG going further than proposing a single snapshot on LIG maximum
4 warmth and thus accounting for asynchronous changes across the globe is due to the difficulty in
5 building robust and coherent age models for different climatic archives during the LIG (Govin et al.,
6 2015). Recently, Capron et al. (2014) have proposed a new climate synthesis for the high latitude
7 regions based on a coherent temporal framework between ice and marine archives. This allows for the
8 first time to assess both the temporal and the spatial evolution of the climate throughout the LIG
9 (Capron et al., 2014).

10 Transient LIG climate simulations provide the possibility to determine when and where maximum
11 LIG warmth occurred, and whether a given record may be seasonally biased or rather represents annual
12 mean temperatures. Therefore, transient climate simulations may help to clarify the origin of the
13 disagreement between model and data. In this study, we analyze the effect of a reduced GIS on LIG
14 global climate with a focus on surface temperature (TS) at 130 kyr BP. The TS is derived from
15 equilibrium simulations performed with an AOGCM. We perform several sensitivity simulations with
16 different boundary conditions and use three different methods of reducing GIS elevation to half its
17 preindustrial elevation and/or extent. This approach enables us to determine what GIS configuration
18 has the strongest impact on the global temperature. Additionally, we assess the importance of additional
19 foreings-like insolation and albedo. Furthermore, in order to validate our results, we perform a model-
20 data comparison using three different proxy-based temperature compilations by CAPE Last Interglacial
21 Project Members (2006), Turney and Jones (2010), and Capron et al. (2014). For model-data
22 comparison, we additionally consider the timing uncertainty on the maximum LIG warmth as
23 determined from our transient simulations as well as the potential seasonal bias of the proxy record.

24 **2. Data and methods**

25 **2.1 Model description**

26 The Community Earth System Models (COSMOS) consist of the general atmosphere circulation model
27 ECHAM5 (5th generation of the European Centre Hamburg Model; Roeckner et al., 2003), the land
28 surface and vegetation model JSBACH (Jena Scheme of Atmosphere Coupling in Hamburg; Raddatz et
29 al., 2007), the general ocean circulation model MPIOM (Max-Planck-Institute Ocean Model; Marsland
30 et al., 2003), and the OASIS3 coupler (Ocean-Atmosphere-Sea Ice-Soil; Valcke et al., 2003; Valcke,

1 2013) that enables the atmosphere and ocean to interact with each other. COSMOS is mainly developed
2 at the Max-Planck-Institute for Meteorology in Hamburg (Germany). The atmospheric component
3 ECHAM5 is a spectral model, which is used in this study at a horizontal resolution of T31
4 ($\sim 3.75^\circ \times 3.75^\circ$) with a vertical resolution of 19 hybrid sigma-pressure levels, the highest level being
5 located at 10 hPa. The JSBACH simulates fluxes of energy, momentum, and CO₂ between land and
6 atmosphere and comprises the dynamic vegetation module by Brovkin et al. (2009), which enables the
7 terrestrial plant cover to explicitly adjust to variations in the climate state. MPIOM is formulated on a
8 bipolar orthogonal spherical coordinate system. We employ it at a horizontal resolution of GR30
9 (corresponding to $\sim 3^\circ \times 1.8^\circ$) with 40 vertical levels. MPIOM includes a Hibler-type zero-layer
10 dynamic-thermodynamic sea ice model with viscous plastic rheology (Semtner, 1976; Hibler, 1979).
11 No flux correction is applied (Jungclaus et al., 2006). Model time steps are 40 min (atmosphere) and
12 144 min (ocean). This COSMOS configuration has been applied for the mid- and early Holocene (Wei
13 and Lohmann, 2012), glacial conditions (Gong et al., 2013; Zhang et al., 2013, 2014), the Pliocene
14 (Stepanek and Lohmann, 2012), the Miocene (Knorr et al., 2011; Knorr and Lohmann, 2014), future
15 climate projections (Gierz et al., 2015), and the LIG (Lunt et al., 2013; Pfeiffer and Lohmann, 2013;
16 Bakker et al., 2014; Felis et al., 2015; Gong et al., 2015; Jennings et al., 2015).

17 **2.2 Experimental setup**

18 As control climate, we use a PI simulation described by Wei et al. (2012). Greenhouse gas
19 concentrations and astronomical forcing of the PI simulation are prescribed according to the
20 Paleoclimate Modelling Intercomparison Project Phase 2 (PMIP2) protocol (Braconnot et al., 2007).
21 Several equilibrium simulations covering the LIG are performed using fixed boundary conditions for
22 130 and 125 kyr BP time slices. The latter simulation is performed in order to assess whether a
23 reduction in GIS at 125 kyr BP improves the agreement between the model and the three proxy
24 compilations considered in this study (CAPE Last Interglacial Project Members, 2006; Turney and
25 Jones, 2010; 125 kyr BP time slice by Capron et al., 2014). Astronomical parameters for the time slices
26 considered in this study have been calculated according to Berger (1978) and are given in Table 1. It is
27 known that one main driver for LIG climate is the Earth's astronomical parameters (Kutzbach et al.,
28 1991; Crowley and Kim, 1994; Montoya et al., 2000; Felis et al., 2004; Kaspar and Cubasch, 2007).
29 During the early part of the LIG, the axial tilt (obliquity) was higher which caused stronger summer
30 insolation at high latitudes of the Northern Hemisphere, while the low latitudes received less insolation;
31 this effect manifests in enhanced seasonality (i.e. warmer summers and cooler winters) in the early LIG

1 climate. The Earth's orbital eccentricity was more than twice the present-day value (Berger and Loutre,
2 1991), and boreal summer coincided with the Earth passing the perihelion (Laskar et al., 2004; Yin and
3 Berger, 2010).

4 Our main focus is the effects of height and extent of the GIS and of insolation changes on climate;
5 consequently, GHG concentrations are prescribed at mid-Holocene levels (278 parts per million by
6 volume (ppmv) CO₂, 650 parts per billion by volume 10 (ppbv) CH₄, and 270 ppbv N₂O, Table 1). An
7 additional simulation is performed using values for GHG concentrations proposed in the Paleoclimate
8 Modelling Intercomparison Project Phase 3 (PMIP3) for the 130 kyr BP time slice (e.g. Lunt et al.,
9 2012) and corresponding to 257 ppmv for CO₂, 512 ppbv for CH₄, and 239 ppbv for N₂O (LIG-GHG,
10 Table 1, Fig. S1). This simulation is included in the Supplementary material as a control run for the
11 GHG concentrations used in our LIG sensitivity simulations, in order to show that there is no large
12 scale impact of lower GHG concentrations relative to our LIG control simulation (Fig. S1). Another
13 LIG simulation is forced with increased CH₄ (760 ppbv) and slightly increased CO₂ (280 ppmv) in
14 order to have one LIG simulation that has identical GHG concentrations to the ones prescribed in the PI
15 simulation (Wei et al., 2012) (Table 1).

16 The size of the GIS during the LIG is not well constrained by reconstructions (Koerner, 1989;
17 Koerner and Fisher, 2002; NGRIP members, 2004; Johnsen and Vinther, 2007; Willerslev et al., 2007;
18 Alley et al., 2010; NEEM Community members, 2013). We take this uncertainty into account and
19 perform sensitivity simulations with three different elevations and two different ice sheet areas of the
20 GIS (Fig. 1). An LIG simulation with a preindustrial GIS elevation (LIG-ctl, Table 1, Fig. 1a) is used
21 as control run for our LIG simulations, which allows us to quantify the exclusive effects of Greenland
22 elevation on climate. Four simulations are performed using a modified GIS (Table 1). We consider (1)
23 GIS lowered to half its preindustrial elevation with unchanged GIS area (LIG-×0.5, Fig. 1b); (2) a GIS
24 lowered by 1300 m (LIG-1300m); at locations where the preindustrial Greenland elevation is below
25 1300 m, we set LIG orography to zero meters, but define the ground to be ice covered and keep the
26 albedo at values typical for the GIS (Fig. 1c); (3) a GIS similar to LIG-1300m, but with albedo
27 adjustment at locations where prescribed LIG orography is zero meters (LIG-1300m-alb); at such
28 locations the land surface is defined as being ice-free and the background albedo is reduced from 0.7 to
29 0.16 (Fig. 1d), an albedo value that is typical for tundra (Fitzjarrald and Moore, 1992; Eugster et al.,
30 2000) – this simulation, in combination with LIG-1300m and LIG-ctl, allows us to separate the climatic
31 effects of a lowered and spatially reduced GIS from those of changes in albedo; (4) a simulation similar

1 to (3), but with an atmospheric concentration of CH₄ that is increased to 760 ppbv (LIG-1300m-alb-
2 CH₄, Fig. 1d); this simulation enables us to quantify the combined effect of a lowered GIS elevation,
3 changes in albedo and insolation with respect to PI.

4 Such changes in GIS elevation and extent would lead to a sea level rise of about 3 m ~~instead of 7 m~~
5 for the present situation due to the post-glacial rebound effect (~~relaxation of the lithosphere~~), when
6 assuming no elastic lithosphere deformation (Fowler, 2004). A sea level change of +3 m is in
7 agreement with other studies that suggest an increase in sea level of 0.3 to 5.5 m during the LIG as a
8 result of GIS melting (Cuffey and Marshall, 2000; Tarasov and Peltier, 2003; Lhomme et al., 2005;
9 Otto-Bliesner et al., 2006; Carlson et al., 2008; Colville et al., 2011; Quiquet et al., 2013; Stone et al.,
10 2013). It is however not compatible with the elevation change inferred from the air content at NEEM
11 (NW Greenland), which suggests less than 400 m elevation (albeit with a large uncertainty) decrease
12 starting from an ice sheet thicker than today at the end of the penultimate deglaciation, and along the
13 last interglacial period (NEEM Community members, 2013).

14 Generally, other boundary conditions of the simulations are kept at their preindustrial state, except
15 for vegetation which is computed dynamically according to the prevailing climate conditions (the only
16 equilibrium simulation that considers fixed preindustrial vegetation is LIG-GHG).

17 Furthermore, we perform one transient model simulation that covers the Holocene (8–0 kyr BP) and
18 four transient simulations of the LIG (130–115 kyr BP). The Holocene transient simulation is included
19 in this study as a control run for the LIG transient simulations, in order to assess the differences and
20 similarities between the present and last interglacial. For the LIG, we apply orography configurations
21 of LIG-ctl, LIG-×0.5, LIG-1300m-alb, and LIG-GHG, respectively. These LIG transient simulations
22 enable us to extract the temperatures at the LIG thermal maximum. The transient simulations are
23 started from a near-equilibrium state, meaning that the climate system is already adjusted to the
24 prescribed forcings, except for the ocean which needs about 3000 years in order to reach an equilibrium
25 state. Performing such long equilibrium simulations is not feasible due to the involved computational
26 effort. Each transient simulation is accelerated by a factor of ten in order to reduce the computational
27 expense. To this end, astronomical forcing is accelerated following the method of Lorenz and Lohmann
28 (2004). The astronomical parameters are calculated after Berger (1978). During the simulations, the
29 ~~tracegreenhouse~~ gas concentrations remain fixed – except for the LIG-GHG-tr, where a timeseries is
30 prescribed according to Lüthi et al. (2008) for CO₂, Loulergue et al. (2008) for CH₄, and Spahni et al.
31 (2005) for N₂O, as proposed for PMIP3. The respective values are interpolated to a 0.01 kyr resolution

1 that corresponds to the accelerated model time axis. A fixed preindustrial vegetation is considered only
2 in the LIG-GHG-tr, in the other transient simulations vegetation is computed dynamically. For the
3 Holocene run, the orography is identical to preindustrial conditions.

4 In order to determine whether TS anomalies between simulations are statistically significant or rather
5 caused by internal variability (noise), we perform an independent two-tailed Student's t test t following
6 Eq. (1). For each grid cell, it relates time averages X and standard deviations σ of model output time
7 series of two given model simulations X_1 and X_2 of a length of n timesteps, in dependence of the
8 effective degrees of freedom (DOF_{eff}). The DOF_{eff} are calculated considering the lag-1 autocorrelation
9 acf (von Storch and Zwiers, 1999):

$$10 \quad \text{DOF}_{\text{eff}} = n(1 - \text{acf}) / (1 + \text{acf}) \quad \text{with} \quad \text{acf} = \max(\text{acf}, 0),$$

11 meaning that the DOF_{eff} cannot be higher than 50, as the last 50 model years of each simulation are
12 used for the analysis. For each grid point from X_1 and X_2 simulations, the smaller DOF_{eff} value is used
13 for calculating the significance value with a 95% confidence interval.

$$14 \quad t = \frac{\bar{X}_1 - \bar{X}_2}{\sqrt{\frac{\sigma^2(X_1)}{n} + \frac{\sigma^2(X_2)}{n}}} \quad (1)$$

15 Surface temperature at locations where the t test t of two data sets indicates a significance value below
16 the critical value is considered to be statistically insignificant and is marked by hatches on geographical
17 maps presented throughout this study.

18 For the analysis of time slice simulations, we define winter and summer as the mean of the 50
19 coldest and warmest months, respectively, for each grid cell, as we are mainly interested in local
20 seasons. In all performed simulations, a modern calendar is assumed. Although in reality the definition
21 of seasons changes over time due to orbital precession ([Joussaume and Braconnot, 1997](#); [Lorenz and](#)
22 [Lohmann, 2004](#)), taking this calendar shift into account would only have a minor influence on our
23 results since we calculate the summer and winter seasons by extracting the warmest and coldest month,
24 respectively. Maximum and minimum LIG TS are calculated from the transient simulations considering
25 the time interval between 130 and 120 kyr BP. In order to filter out internal variability, a 100-point
26 running average representing the average over 1000 calendar years is applied. Maximum and minimum
27 LIG warmth of the summer are defined as the warmest and coldest average of 100 warmest months,
28 respectively, which reflects the warmest or coldest 1000 summer seasons with respect to the

1 astronomical forcing. For the maximum and minimum LIG warmth of annual mean, we consider the
2 warmest and coldest average of 100 model years, respectively. The seasonality range is defined by
3 calculating the summer maximum LIG warmth (warmest average of 100 warmest months of the model
4 years) and winter minimum LIG TS (coldest average of 100 coldest months of the model years).

5 **2.3 Temperature reconstructions**

6 In order to test the robustness of our simulations, we additionally perform a model-data comparison
7 using proxy-based temperature anomalies that are available for the northern high latitudes (CAPE Last
8 Interglacial Project Members, 2006), across the globe (Turney and Jones, 2010), and in middle to high
9 latitudes (Capron et al., 2014). The temperature reconstructions from CAPE Last Interglacial Project
10 Members (2006) are based on terrestrial and marine proxy records and estimate summer temperatures
11 for maximum LIG warmth relative to PI. The global dataset by Turney and Jones (2010) comprises
12 terrestrial and marine proxy records and estimates annual mean temperatures for maximum LIG
13 warmth (terrestrial) and for the period of **plateaued/levelled** $\delta^{18}\text{O}$ (marine), relative to present day (PD,
14 1961–1990; Smith and Reynolds, 1998; New et al., 1999). The high latitude climate synthesis by
15 Capron et al. (2014) provides temporal air and sea surface temperature (SST) reconstructions based on
16 ice core and marine records respectively, across the interval 115 to 130 kyr BP (in our study covering
17 the period between 125 and 115 kyr BP). They also propose snapshots of surface temperature
18 anomalies and associated quantitative uncertainties at 115, 120, 125 and 130 kyr BP, but here we use
19 the last two snapshots. Detailed information regarding the proxy data is given in CAPE Last
20 Interglacial Project Members (2006), Turney and Jones (2010), and Capron et al. (2014), respectively.

21 In order to quantify the agreement between model and data, we calculate the root-mean-square
22 deviation (RMSD) which is a measure of the differences between an estimator (y_{model}) and estimated
23 parameter (y_{data}) (Gauss and Stewart, 1995; Mudelsee, 2010). RMSD is defined in Eq. (2):

$$24 \quad \text{RMSD} = \sqrt{\frac{1}{n} \sum_{i=1}^n (y_{\text{model}} - y_{\text{data}})^2} \quad (2)$$

25 where y_{model} is the simulated TS anomaly at the location of the proxy record, y_{data} indicates the
26 reconstructed TS anomaly, and n is the number of data samples.

27 **3. Results**

28 In the first part of this section, we present results from our LIG GIS sensitivity simulations, focusing on
29 TS anomalies. Afterwards, a short description of results from the transient simulations is presented,

1 followed by the model-data comparison and consideration of potential uncertainties in the data.

2 **3.1 Greenland Ice Sheet elevation and albedo influence on global surface** 3 **temperature**

4 **3.1.1 Annual mean anomalies**

5 Figure 2 ~~presentsshow~~s the ~~the global effect on~~ TS ~~changes~~ of lowering ~~the~~ GIS ~~half its preindustrial~~
6 ~~elevation by~~ by various methods. We observe the strongest warming over Greenland (of up to +12.5°C)
7 in the LIG-1300m-alb (Figs. 1c and 2c). Northern North America and the Arctic Ocean warm by up to
8 +2°C in all GIS sensitivity simulations. A pronounced warming is found over the southernmost
9 Southern Ocean of up to +4°C (Fig. 2a–c).

10 Considering all LIG sensitivity simulations, the highest TS mean anomalies globally and in the
11 (global mean-Southern Hemisphere-TS anomaly) is are simulated in LIG-1300m-alb, with an average of
12 $\Delta TS = +0.37^\circ\text{C}$ and ($\Delta TS = +0.31^\circ\text{C}$, respectively) (Table 2). However, for the Northern Hemisphere,
13 the highest average TS anomaly of $\Delta TS = +0.47^\circ\text{C}$ is found in LIG- $\times 0.5$ (Table 2). Consequently, the
14 exact method of changing GIS configuration influences the hemispheric temperature anomalies.

15 The most affected areas by changes in GIS configuration are the northern high latitudes, which
16 experience a warming of $\Delta TS = +1.45^\circ\text{C}$ in LIG-1300m-alb, and $\Delta TS = +1.07^\circ\text{C}$ and $\Delta TS = +1.03^\circ\text{C}$
17 in LIG- $\times 0.5$ and LIG-1300m, respectively. This indicates that albedo plays a significant role in the
18 ~~northern high latitude~~-temperature changes over northern high latitudes, where it is causing an average
19 temperature anomaly of $\Delta TS = +0.42^\circ\text{C}$. A local cooling of up to -1.60°C is limited to the Barents Sea
20 in LIG- $\times 0.5$ and LIG-1300m (Fig. 2a, b), south-west of Greenland in LIG-1300m (Fig. 2b), and a
21 cooling of up to -2.30°C over the Sea of Okhotsk (western Pacific Ocean) in LIG-1300m-alb caused
22 by a reduction in albedo in the prescribed ice-free areas (Fig. 2c, d). In the latter simulation, the Barents
23 Sea cooling is counteracted by a warming caused by changes in albedo (Fig. 2d).

24 At 130 kyr BP, the AMOC was reduced by 3.5 Sv as compared to the PI (Table 2). However, a
25 reduction in GIS partly counteracts the negative anomaly and leads to a smaller reduction of AMOC
26 (3.5-2.2=1.3 Sv) relative to the PI an increase in the AMOC of up to 2.2 Sv relative to LIG-eti (Table 2).
27 After performing an independent two-tailed Student's t test t with 95% confidence interval, we find that
28 these changes in AMOC are statistically significant.

29 **3.1.2 Winter and summer mean anomalies**

30 The seasonal effect of a reduced GIS elevation is strongest during local winter in both hemispheres in

1 all GIS sensitivity simulations (Table 2). However, for simplicity we focus here only on the GIS
2 sensitivity simulation that includes changes in GIS elevation and corresponding changes in albedo
3 (LIG-1300m-alb, Fig. 3). In the Northern (Southern) Hemisphere, winter TS changes by $\Delta TS =$
4 $+0.57^{\circ}\text{C}$ ($\Delta TS = +0.39^{\circ}\text{C}$), with the northern high latitudes ($60\text{--}90^{\circ}\text{N}$) experiencing the highest positive
5 anomalies of $\Delta TS = +2.08^{\circ}\text{C}$ (Fig. 3a, Table 2).

6 During summer, the TS anomaly is also positive but of lower magnitude, with an average of $\Delta TS =$
7 $+0.24^{\circ}\text{C}$ for Northern Hemisphere, Southern Hemisphere, and globally (Fig. 3b, Table 2). The northern
8 high latitudes warm during summer by $\Delta TS = +0.46^{\circ}\text{C}$, which is a modest change compared to winter
9 warming. Relatively strong cooling occurs over the Sea of Okhotsk and south-west of Greenland (Fig.
10 3), again with the strongest effect being present during winter.

11 **3.2 Combined effects of LIG forcings on global surface temperature**

12 The combined effects on TS of reducing the GIS by 1300 m, adjusting albedo, and applying
13 astronomical changes that represent an LIG climatic setting are presented in Fig. 4. Assuming linearity
14 of the different climatic drivers, we can additionally split the anomaly of PI and LIG-1300m-alb-CH₄
15 (equivalent to LIG-1300m-alb, but with a CH₄ concentration adjusted to PI simulation) into the isolated
16 contributions of changes in elevation and albedo and in astronomical forcing (calculated as the
17 difference between the anomaly of LIG-1300m-alb-CH₄ and PI, and the anomaly of LIG-1300m-alb
18 and LIG-ctl).

19 Considering the TS values from Table 2, we find that the magnitude of the astronomical forcing
20 influence is stronger than the effects of lowering the GIS and respective adjustment of the albedo in the
21 global average of annual mean TS, as well as the annual mean average over Northern Hemisphere (Fig.
22 4a). In the Southern Hemisphere, both forcings have equal contributions to changes in annual mean TS
23 (Fig. 4a). During winter, changes in GIS have the strongest influence globally and in the Northern
24 Hemisphere, while in the Southern Hemisphere changes in astronomical forcing are dominant (Fig. 4b).
25 During summer, there is an opposite pattern (Fig. 4c). The strongest combined effect of insolation and
26 changes in GIS and albedo occurs in the Northern Hemisphere during summer with an anomaly of ΔTS
27 $= +2.51^{\circ}\text{C}$. Globally, the combined effect leads to a warming of $\Delta TS = +1.34^{\circ}\text{C}$ during summer. In the
28 Southern Hemisphere, the strongest combined effect is simulated during winter with $\Delta TS = +1.08^{\circ}\text{C}$.

29 The winter (local minimum TS) of the LIG is in general cooler than the PI at northern low to
30 middle latitudes, while at northern high latitudes and Southern Hemisphere winter is warmer (Fig. 4b).
31 If we separate the astronomical effect from the GIS lowering and albedo changes, we can attribute to

1 insolation a cooling of $\Delta TS = -0.52^{\circ}\text{C}$ in Northern Hemisphere, and a warming of $\Delta TS = +0.69^{\circ}\text{C}$ in
2 Southern Hemisphere.

3 Summer (local maximum TS) anomalies of the LIG with respect to PI are stronger than winter
4 anomalies in the Northern Hemisphere (Fig. 4c). Strongest continental summer TS anomalies are
5 located in the Northern Hemisphere (up to $\Delta TS = +16.7^{\circ}\text{C}$). Locations where the LIG is cooler than PI
6 are found at $\sim 10^{\circ}\text{N}$ over Africa and at $\sim 25^{\circ}\text{N}$ over India.

7 **3.3 Surface temperature evolution during the present and Last Interglacial**

8 In Figs. 5, S2, and S3, a comparison of transient TS derived from the five transient simulations (Table
9 1) is shown. The LIG transient simulations are important for determining when the maximum LIG
10 warmth occurred ~~in-dependence~~ as a function of the location as well as seasons. The TS evolution in the
11 northern high latitudes ($60\text{--}90^{\circ}\text{N}$) is displayed in Fig. 5. All LIG (130–115 kyr BP) simulations (LIG-
12 ctl-tr, LIG- $\times 0.5$ -tr, LIG-1300m-alb-tr, and LIG-GHG-tr) indicate a similar annual mean trend, starting
13 with a plateau until mid-LIG (around 123 kyr BP) followed by a pronounced cooling trend (Fig. 5a).
14 The LIG-ctl-tr starts at a slightly higher TS than the LIG-GHG-tr, but although the trace gas
15 concentrations are mostly lower throughout the latter, the LIG-GHG-tr simulates higher TS throughout
16 the LIG. This indicates that changes in the vegetation which are simulated in the LIG-ctl-tr lead to a
17 cooling in the Northern Hemisphere, partly counteracting the warming induced by higher GHG
18 concentrations. The most extreme case is represented by LIG-1300m-alb-tr, which shows
19 predominantly the highest TS relative to TS of other LIG transient simulations. The Holocene (8–0 kyr
20 BP) transient simulation (HOL-tr) starts also with a warming until around mid-Holocene (6 kyr BP),
21 followed by a cooling trend.

22 During winter, all LIG simulations indicate a positive trend in the early LIG, with maximum TS at
23 around mid-LIG (Fig. 5b), followed by a strong cooling. The relative order of magnitudes of TS trends
24 during different simulations is the same as for annual mean TS, but with a relatively larger offset in
25 between simulations. Simulation HOL-tr shows a warming, followed by a cooling trend that starts at
26 mid-Holocene (Fig. 5b). Winter TS are characterized by stronger temporal variability than summer TS
27 (Fig. 5b, c). Summer TS in all LIG simulations indicate a slight warming trend until around 128 to 126
28 kyr BP, followed by a pronounced cooling. The offset between transient TS is smaller than for annual
29 mean and winter, but with the same order on the temperature scale. A dramatic cooling is also present
30 in the Holocene simulation starting at mid-Holocene (Fig. 5c). Furthermore, the timing of the
31 maximum LIG warmth does not occur simultaneously between the winter and summer seasons, the

1 winter season indicating a later peak than summer (Figs. 5, S2, and S3).

2 **3.4 Comparison of model results to temperature reconstructions**

3 Due to the large amount of simulated data, we display in the model-data comparison simulated LIG TS
4 derived from only one equilibrium simulation with changes in GIS, namely LIG-1300m-alb. For the
5 calculation of the maximum LIG warmth, we consider the corresponding transient simulation (LIG-
6 1300m-alb-tr). However, the comparison of the proxy-based temperatures with the other GIS
7 sensitivity simulations is considered in Table S1 in the Supplementary material, which gives the RMSD
8 values between temperature reconstructions and simulated TS extracted at the location of each given
9 proxy record and derived from simulations with different GIS boundary conditions. Furthermore, we
10 display also results from control simulation for 130 kyr BP (LIG-ctl) and the corresponding transient
11 simulation (LIG-ctl-tr) for maximum LIG warmth, in order to determine if and where GIS changes lead
12 to an increase in model-data agreement.

13 **3.4.1 Proxy-based summer temperature reconstructions**

14 Figures 6, 8a, and S4a present a model-data comparison that consider LIG terrestrial and marine proxy-
15 based summer temperature anomalies relative to PI derived by CAPE Last Interglacial Project
16 Members (2006). Simulated and reconstructed temperature anomalies agree reasonably well with
17 respect to the sign of the change, in the simulation with a reduction in GIS (LIG-1300m-alb, Fig. 6a)
18 and with preindustrial GIS configuration (LIG-ctl, Fig. 6c). The best agreement between model and
19 proxy reconstructions occurs over northern Asia and Europe. In the North Atlantic Ocean and the Arctic
20 Ocean, the model underestimates the magnitude of change indicated by the marine-based temperature
21 reconstructions (Fig. 6a, c). However, a reduction in GIS and albedo leads to slightly higher summer
22 temperature anomalies at the location of some marine proxies in the North Atlantic Ocean, partly
23 reducing the model-data mismatch (Fig. 6a). Over Greenland, the elevation changes lead to an
24 overestimation of the reconstructed temperature anomalies – proxy records show anomalies of +4 to
25 +5°C, while the simulated TS anomalies are above +7°C (Fig. 6a). However, in the LIG-ctl, there is an
26 underestimation of the magnitude of change indicated by the reconstructed temperatures (Fig. 6c).

27 In the case of the terrestrial proxies, the temperature span covers +2 to +6°C, while the
28 corresponding simulated anomalies cover +1 to +11°C. In addition to the 130 kyr BP simulation (LIG-
29 1300m-alb), for each given core location we also consider TS anomalies relative to PI calculated at the
30 minimum and maximum LIG summer warmth as derived from the LIG-1300m-alb-tr (Fig. 8a). In
31 about half the cases (14 records out of 27), the error bars touch the 1 : 1 line, possibly indicating better

1 agreement than when compared to summer TS anomalies at 130 kyr BP (Fig. 8a). However, the number
2 of 13 unresolved records can be reduced to 11, when the terrestrial proxy-based temperature anomalies
3 are compared to the LIG-ctl-tr (Fig. S4a). Marine-based temperature anomalies and the corresponding
4 simulated anomalies (from LIG-1300m-alb) cover temperature spans of 0 to +3°C and of ~0 to +4°C,
5 respectively (Fig. 8a). Seven out of thirteen marine records cannot be reconciled with the simulations
6 when considering maximum and minimum summer TS anomalies during the LIG (Figs. 8a and S4a).
7 When the reconstructed data is compared to simulated annual mean TS anomalies at 130 kyr BP (Figs.
8 S5a, c and S6) and at annual mean minimum or maximum LIG warmth (Figs. S5b, d and S6), we find
9 an even higher discrepancy than when compared to the summer average, implying that the
10 reconstructed records are indeed biased towards summer, when assuming that the model is realistic.

11 The proxy dataset by CAPE Last Interglacial Project Members (2006) is considered to represent
12 summer temperatures at the maximum LIG warmth. Thus, we additionally include in the model-data
13 comparison the simulated maximum LIG warmth calculated from our transient LIG simulations (Fig.
14 6b, d). We find that the agreement between model and data increases in some cases. For the northern
15 North Atlantic Ocean, for example, marine records agree best with simulated TS anomalies at the
16 maximum LIG warmth (between 121.5 and 124.5 kyr BP, Fig. 9a) in the LIG-1300m-alb (Fig. 6b).
17 However, the RMSD between the simulated TS and reconstructed temperature anomalies reveals that
18 the best agreement occurs with TS anomalies at maximum LIG warmth in the LIG-ctl-tr (Table S1 in
19 Supplementary material). A reduction in GIS, thus, does not improve in general the model-data
20 agreement when the dataset by CAPE Last Interglacial Project Members (2006) is considered.
21 However, changes in GIS lead to high temperature anomalies during local winter (Fig. 3a), while
22 summer season is not strongly influenced (Fig. 3b). Therefore, in a comparison with proxy
23 reconstructions that represent summer temperature anomalies, changes in GIS do not have a significant
24 impact on model-data agreement.

25 **3.4.2 Proxy-based annual mean temperature reconstructions**

26 Both reconstructed (Turney and Jones, 2010) and simulated global annual mean temperature
27 anomalies indicate that the high latitudes experienced warmer temperatures during the LIG than in the
28 PI, with strongest anomalies being present in the northern high latitudes (Fig. 7). However, the model
29 underestimates the strong positive anomalies derived from proxy records, and in low and middle
30 latitudes the model cannot capture the magnitude of the cooling that the proxy records show (Figs. 7a,
31 c, 8b, and S4b).

1 Changes in GIS have no significant influence in low to middle latitudes but cause strong positive
2 anomalies in the northern high latitudes thus improving the model-data comparison (Fig. 7a, Table S2),
3 although the model still underestimates the proxy amplitude of the signal depicted by reconstructions.
4 Terrestrial proxy records indicate stronger anomalies with $\Delta TS = +2.21^\circ\text{C}$ (globally), $\Delta TS = +2.21^\circ\text{C}$
5 (Northern Hemisphere), and $\Delta TS = +2.11^\circ\text{C}$ (Southern Hemisphere). The corresponding simulated
6 anomalies indicate a global average of $\Delta TS = +1.44^\circ\text{C}$, underestimating the temperature change
7 indicated by the records by $\sim 1^\circ\text{C}$. The Northern Hemisphere and Southern Hemisphere average TS
8 anomalies are $\Delta TS = +1.48^\circ\text{C}$ and $\Delta TS = +0.92^\circ\text{C}$, respectively. Marine records capture lower
9 anomalies than their terrestrial counterparts but still larger anomalies than the corresponding simulated
10 anomalies.

11 The majority of the terrestrial records shows a stronger signal than the simulated anomalies (Fig. 8b).
12 The temperature anomaly range in the terrestrial reconstructed data covers -5 to $+15^\circ\text{C}$, while the
13 model covers 0 to $+12^\circ\text{C}$. Out of 100 terrestrial records, 33 agree with the simulated TS anomalies
14 somewhere between the annual mean minimum and maximum LIG warmth derived from LIG-1300m-
15 alb-tr (Fig. 8b), and 19 records with simulated TS anomalies derived from LIG-ctl-tr (Fig S4b).

16 The reconstructed marine temperature anomalies cover a range of -6 to $+11^\circ\text{C}$ compared to 0 to
17 $+3^\circ\text{C}$ in the model, indicating pronounced underestimation of the marine proxy-based anomalies by the
18 model (Figs. 7a and 8b). When we consider both annual mean minimum and maximum LIG warmth,
19 the simulated TS span increases by $\sim 1^\circ\text{C}$ (-0.5 to $+3.5^\circ\text{C}$). Twenty records (out of 162) agree with the
20 model data somewhere between the minimum and maximum LIG warmth with respect to annual mean
21 derived from LIG-1300m-alb-tr, and 25 records when LIG-ctl-tr is considered (Fig. S4b).

22 The proxy records derived by Turney and Jones (2010) are considered to record an annual mean
23 temperature signal. Nevertheless, some records may be biased towards a specific season. Therefore, we
24 also consider the minimum winter and maximum summer TS during the LIG (Fig. 4c). Seasonality
25 increases the span of the vertical bars, providing the possibility of a better agreement with the
26 reconstructed temperature anomalies. The agreement between proxy records and model simulations
27 increases, with 51 (69) terrestrial and 53 (51) marine records being reconciled by considering
28 seasonality derived from LIG-1300m-alb-tr (LIG-ctl-tr) (Figs. 4c and S4c).

29 As already mentioned, the terrestrial proxy records by Turney and Jones (2010) are considered to
30 record annual mean temperature anomalies at the maximum LIG warmth. Therefore, we additionally
31 compare the terrestrial records with the simulated annual mean at the LIG thermal maximum (Fig. 7b,

1 d). Over Europe, the agreement between model and data is increased for those records that indicate a
2 warming, since the simulated anomalies derived from LIG-1300m-alb-tr indicate a warming at the
3 maximum LIG warmth, while presenting nearly no change at 130 kyr BP (Fig. 7a). A better agreement
4 is found also over northern Asia. According to Table S2, the terrestrial proxy-based temperature
5 anomalies indicate the best agreement with the simulated annual mean TS at the maximum LIG
6 warmth derived from the LIG-1300m-alb. The annual mean anomalies are influenced by winter
7 temperatures, the season during which GIS leads to strong positive anomalies. Therefore, a model-data
8 comparison with proxy reconstructions that represent an annual mean signal shows a better agreement
9 than when summer proxies are considered.

10 **3.4.3 Time resolved proxy-based summer temperature reconstructions**

11 For a more robust model-data comparison, we additionally compare our simulated TS to a compilation
12 of high-latitude LIG temperature anomalies derived from synchronized records representing 130 kyr
13 BP (Figs. 10 and S12, Capron et al., 2014). The synchronization is performed by aligning marine
14 sediment records onto the recent AICC2012 ice chronology (Capron et al., 2014 and references
15 therein). This method reduces the uncertainty in relative dating of the proxy reconstructions. The
16 marine records from the North Atlantic Ocean indicate mostly negative anomalies, while the model
17 simulates nearly no changes. The melting of the remnant Northern Hemisphere ice-sheets from the
18 penultimate glaciation leads to a cooling of the North Atlantic Ocean (Stone et al., 2016), a factor that
19 is not considered in our simulations, which indicate only a modest change in this region. As shown
20 above, GIS reduction leads to a small increase in summer TS anomalies, thus increasing the model-data
21 disagreement (Figs. 10a and S12a). A warming in the Southern Ocean is captured by both the model
22 and proxies, though the model underestimates the amplitude of the signal when compared to
23 reconstructions. Reducing the GIS and albedo leads to an increase in local summer TS anomalies in the
24 Southern Ocean bringing the model and data in slightly closer agreement (Figs. 10b and S12b).

25 Considering Table S3, the reconstructed temperatures agree best with the simulated summer TS at
26 125 kyr BP in LIG-125k (Fig. S15), which considers a reduced GIS configuration (as in the LIG-
27 1300m-alb), both indicating a warming. However, this result is not conclusive with respect to the GIS
28 elevation, as a simulation with preindustrial GIS elevation has not been yet performed for this
29 particular time slice. For 130 kyr BP, the best agreement occurs for the LIG-ctl but for annual mean
30 rather than summer, since the model simulates an annual mean cooling in the North Atlantic Ocean
31 (Fig. S5c).

1 A model-data comparison of LIG temperature trends is also considered in our study (Figs. S13 and
2 S14). The proxy-based temperature trends by Capron et al. (2014) is compared to the temperature
3 evolution derived from our transient simulations (LIG-ctl-tr and LIG-1300m-alb-tr), between 125 and
4 115 kyr BP. ~~Depending on the location, An underestimation or overestimation of the signal depicted~~
5 ~~by the proxy records in our simulation is again identified, as well as an overestimation depending on~~
6 ~~the location of the proxies by the model is again found~~ (Figs. S13 and S14). Changes in GIS do not
7 strongly influence the results, with the exception of a few locations where such changes lead to a less
8 pronounced warming simulated in LIG-ctl-tr, thus reducing the mismatch.

9 **4. Discussion**

10 **4.1 Effects of insolation and Greenland Ice Sheet elevation on surface** 11 **temperature**

12 The main focus of our study is to quantify the possible contribution of reduced GIS elevation in
13 comparison with the contribution of insolation forcing to the climate of the LIG.

14 We can confirm the importance of insolation for the Northern Hemisphere, especially for the
15 northern middle to high latitudes (Figs. 4, 6, 7, 10). The belt of decreased TS, observed around 10°N
16 over Africa and 25°N over Arabian Peninsula and India (Figs. 4a, b and 7a), is related to increased
17 cloud cover (Fig. S9) and increased summer precipitation of up to +6 mm d⁻¹ (not shown). This effect
18 has been described by Herold and Lohmann (2009), who propose a mechanism for the temperature
19 anomalies that relies on changes in insolation in conjunction with increased cloud cover and increased
20 evaporative cooling.

21 In general, and independent of GIS elevation, we observe an annual mean global warming of $\Delta TS =$
22 +0.44°C in our LIG simulations relative to PI, hinting to positive feedbacks (such as sea ice-albedo)
23 that amplify the high latitude insolation signal (Fig. 4).

24 In Section 3.1.2, we have shown that the most pronounced impact of reduced GIS elevation (in
25 LIG-1300m-alb) occurs during local winter in both hemispheres (Fig. 3a). The winter warming of up to
26 +3°C over the Arctic Ocean may be linked to a decrease in sea ice and a delayed response to a warming
27 occurring in October (not shown), which is caused by positive sea-ice-albedo feedbacks. A systematic
28 analysis of insolation-driven feedbacks (e.g. sea ice, water vapors, clouds) has been done by Masson-
29 Delmotte et al., 2011. A decrease in albedo over Greenland has the strongest influence during summer
30 especially over the southernmost region (Figs. 2d and 3b), caused by insolation absorption by the ice-

1 free land surface. Furthermore, we note cold annual mean anomalies in the Barents Sea (Fig. 2a, b) and
2 Sea of Okhotsk (Fig. 2c) caused by an increase in sea ice cover.

3 | The change in the GIS elevation also leads ~~also~~ to a relatively strong warming in the southern high
4 latitudes, mainly off the coast of Antarctica, with the strongest positive anomaly occurring during local
5 winter (Fig. 3a) that coincides with a heat flux transfer anomaly from the ocean to the atmosphere (not
6 shown). Increased ocean heat flux during winter leads to a warming of the atmosphere. The Antarctic
7 warming is most likely related to warmer deep water as well as subsurface warming poleward of 50°N
8 in the North and South Atlantic Ocean. The warming may be attributed to enhanced AMOC (Table 2),
9 which plays an important role in the exchange of heat between the hemispheres and between
10 atmosphere and ocean. Our results indicate a weaker AMOC during the LIG as compared to the PI of
11 up to 3.5 Sv, but changes in GIS lead to an increase of up to 2.2 Sv (Table 2). The simulated increase in
12 AMOC in the sensitivity simulations may be triggered by increased salinity of up to + 1 psu in the
13 northern North Atlantic Ocean. Increased salinity cannot be explained by changes in precipitation
14 minus evaporation, which show positive anomalies in this area (not shown). Another contributing
15 factor to the enhanced AMOC may be an increase in the atmospheric flow due to a reduction in GIS
16 elevation. The low pressure system over Greenland and the high pressure system above Europe become
17 more extreme, enhancing the north-eastward air circulation (Fig. 11). We find that the higher the sea
18 level pressure (SLP) anomaly (Fig. 11), the stronger the AMOC (Table 2). This change could also
19 explain the positive TS anomalies of up to +1°C in the northern North Atlantic Ocean, with more heat
20 being transported poleward from the low latitudes (Fig. 2a–c). However, convection cannot be the only
21 explanation for the southern high latitudes warmth, since the heat would be dispersed towards the
22 Southern Hemisphere. We however note a large scale warming in the subsurface of the Southern Ocean
23 which is probably caused by positive feedbacks. This warming may be related to changes in the water
24 stratification. We observe an invigorated vertical mixing in the northern North Atlantic Ocean and a
25 suppressed vertical mixing in the Southern Ocean (not shown), the latter causing the heat at subsurface
26 to be preserved. The Southern Ocean has a large heat capacity leading to a long memory of the system.
27 Lags of up to three months occur in the surface layer including sea ice (amplifying factor via positive
28 ice-albedo and ice-insulation feedbacks), while long-term lags occur in deeper levels below the summer
29 mixed layer that store seasonal thermal anomalies (Renssen et al., 2005).

30 | In contrast to our results that show an increase in the AMOC relative in response to GIS elevation
31 changes, Otto-Bliesner et al. (2006) and Bakker et al. (2012) find a weakening of the AMOC. Bakker et

1 al. (2012) infer that the AMOC is weaker by up to 14 % in a regional study of LIG climate of the North
2 Atlantic Ocean, prescribing a reduction of GIS elevation (by 700 m) and extent (reducing the ice
3 volume by 30%). The weakening of the AMOC is caused by additional freshwater runoff resulting
4 from a melting GIS, a factor that is not considered in our study and that would probably cancel out or
5 reduce the effect of changes in the atmospheric transport on the AMOC. In the study by Bakker et al.
6 (2012) using a simplified atmosphere model, reducing GIS elevation and extent leads to changes in the
7 atmospheric flow pattern and creates a special pattern of surface pressure anomalies. In particular in the
8 Norwegian Sea, Barents Sea, and south-east of Greenland, the low pressure system is weaker,
9 inhibiting the overturning circulation.

10 The reduction of the GIS elevation and albedo alone leads in the study by Bakker et al. (2012) to a
11 local warming of up to +4°C in July, a substantially lower anomaly (factor of ~3) than simulated in our
12 model for local summer when reducing both GIS and albedo. However, when comparing their
13 simulated data to proxy-based temperature anomalies relative to PI (CAPE Last Interglacial Project
14 Members, 2006), Bakker et al. (2012) find an overestimation of the magnitude of temperature change
15 recorded by reconstructions over Greenland, and an underestimation at eastern Europe and Baffin
16 Island – locations where we find a similar temperature tendency (Fig. 6a).

17 Another climate model study that considers a reduction in GIS topography by various methods has
18 been performed by Merz et al. (2014). In their GIS sensitivity simulations, performed with the
19 Community Climate System Model version 4 (CCSM4), they find a rather mixed signal in temperature
20 anomalies over Greenland relative to the predominant warming found in our simulations with changes
21 in GIS. During local winter, their model simulates a warming of up to +5°C in central Greenland and a
22 cooling of up to -12°C in areas that become flat and ice-free. However, changes in topography of GIS
23 do not have a significant influence on climate in the surrounding areas in the study by Merz et al.
24 (2014). This may be caused by the fact that in their simulations SSTs are prescribed, while in our study
25 the atmosphere model is interactively coupled to an ocean general circulation model. However, in their
26 study the GIS is reconstructed by means of high resolution ice sheet models, while we consider a
27 relatively simplistic representation of the GIS. Differences are found also with respect to changes in
28 low-level winds. They find a rather local influence of the GIS changes and no major effect on the large-
29 scale atmospheric circulation. Our model simulates an enhancement of low-level winds around GIS and
30 on SLP (Fig. 11). As such, the methods of reducing GIS and the model used have a strong influence on
31 the local and large-scale climate. Note, however, that the aims of our study and the study by Merz et al.

1 (2014) are different, since the latter focuses on local effects above Greenland, while our main focus is
2 on the GIS effects on large-scale climate.

3 **4.2 Surface temperature evolution during the Last Interglacial and the** 4 **Holocene**

5 Although our results are not directly comparable to those derived by Bakker et al. (2013), who analyze
6 transient LIG January and July temperature anomalies (simulated by seven different models) with
7 respect to PI while we use transient absolute TS for coldest and warmest month, the pattern of the
8 temperature evolution remains the same. We observe similarities in middle latitudes and in winter
9 temperatures at high latitudes characterized by a large variability, and also note a clear cooling trend for
10 summer caused by a decrease in summer insolation. At northern high latitudes, Bakker et al. (2013)
11 find July maximum LIG warmth at 128.4–125.1 kyr BP, while in middle latitudes the maximum occurs
12 at 129.4–126.3 kyr BP. We also observe a warmest month maximum at around 128 kyr BP for high and
13 middle latitudes. A July maximum LIG warmth is found in the study by Loutre et al. (2014) at 128 kyr
14 BP. They find that the summer SST during the LIG is smaller in the model than in the reconstructed
15 temperatures, especially in the North Atlantic Ocean, but taking into account the evolution of the
16 Northern Hemisphere ice sheets reduces the disagreement between model and data.

17 During winter, our simulations produce a clear high latitude TS maximum around mid-LIG, while
18 the middle latitudes experience peak warmth around 121–117 kyr BP. Bakker et al. (2014) compare
19 transient LIG and Holocene (8–0 kyr BP) temperature trends simulated by different models (including
20 our COSMOS LIG-GHG-tr and HOL-tr simulations). They find negative warmest month temperature
21 trends for both LIG and Holocene in the Northern Hemisphere. Bakker et al. (2013) find a linear
22 relation between changes in insolation and temperatures for both summer and winter and for all
23 latitudes. There are however some exceptions. In northern high-latitudes, the winter temperature
24 changes result mainly from sea-ice related feedbacks and are described as highly model-dependent. In
25 southern middle to high latitudes, winter temperatures are strongly affected by changes in GHG
26 concentrations. Comparing all LIG transient simulations with the Holocene in the three considered
27 latitudinal bands, we observe that the Holocene experiences mostly lower TS than during the LIG, and
28 is characterized by smaller trends.

29 In our LIG transient simulations, we find that the differences in TS between the different model
30 simulations at the beginning of the LIG (130 kyr BP) are higher than during the late LIG (115 kyr BP),
31 indicating that the impact of a reduced GIS is stronger at the beginning of the LIG as compared to

1 glacial inception (GI, 115 kyr BP), possibly related to an interplay with insolation forcing. By using
2 different approaches to simulate the LIG evolution, we offer a bandwidth of possible temperatures, in
3 our model-data comparison, at each given time between 130 and 115 kyr BP.

4 **4.3 Model-data comparison**

5 In combination with changes in the GIS elevation and lower albedo, the insolation effect leads to high
6 positive summer TS anomalies in the Northern Hemisphere (Figs. 4c and 6a). The pattern of these
7 changes is observed also in another model study of the LIG that includes a reduction in GIS elevation
8 of 500 m (Otto-Bliesner et al., 2006). The study shows that the June-July-August (JJA) temperature
9 anomaly with respect to PI is positive in the Northern Hemisphere, especially over the continents – yet,
10 the magnitude of these changes is smaller than in our study. In order to validate their results, Otto-
11 Bliesner et al. (2006) compare the simulated temperature anomalies to proxy-based temperature
12 anomalies by CAPE Last Interglacial Project Members (2006). Comparing our model results to the
13 same proxy compilation, we see most similarities in the local summer, although at some locations the
14 magnitude differs. Over Greenland, the warming reaches +5°C according to the proxy reconstructions,
15 while our results show a higher warming caused by the reduction of the GIS. However, the results from
16 Otto-Bliesner et al. (2006) indicate an underestimation. This suggests that the GIS elevation during the
17 LIG may have not been so drastically reduced as prescribed in our model setup, but was still reduced
18 by at least 500 m. This conclusion is supported by another model-data comparison study (Stone et al.,
19 2013) that uses the same data compilation (CAPE Last Interglacial Project Members, 2006). In their
20 simulation produced with an AOGCM, Stone et al. (2013) find a good agreement between model and
21 reconstruction as well, but cannot capture the reconstructed strong warming over Greenland, where
22 their simulation indicates a warming of up to +3.5°C. They imply that the GIS was reduced in the
23 LIG as compared to PI, but not completely deglaciated – in the simulation with a completely removed
24 GIS, they find much stronger temperature anomalies over Greenland of up to +16°C, higher than in our
25 findings when GIS is reduced to half its present elevation (Fig. 2). A high overestimation of the
26 magnitude of the reconstructed-temperature changes by the model is found also by Otto-Bliesner et al.
27 (2006) for a deglaciated Greenland, with summer temperature anomalies being higher than +10°C.
28 Although in our simulations we do not completely remove the ice sheet, we find strong TS anomalies
29 of up to +11°C.

30 A warming as high as $+8 \pm 4^\circ\text{C}$ is proposed by NEEM Community members (2013) for the peak
31 LIG warmth at 126 kyr BP, based on North Greenland Eemian Ice Drilling (NEEM) ice core. They

1 propose that the northwest GIS is characterized only by a modest reduction of 400 ± 250 m between
2 128 and 122 kyr BP. In our study, we find at the location of the NEEM ice core an annual mean
3 warming of $+9.6^\circ\text{C}$ at 125 kyr BP at a GIS height of 553 m, a warming that is within the temperature
4 range proposed by NEEM Community Members (2013). When the temperature estimate from NEEM
5 ice core is not corrected for elevation changes, it indicates a positive anomaly of $7.5 \pm 1.8^\circ\text{C}$. Such
6 dramatic temperature changes at the NEEM site are proposed by another recent study based on ice core
7 air isotopic composition ($\delta^{15}\text{N}$) and relationships between accumulation rate and temperature (Landais
8 et al., 2016). Their study suggests anomalies between the LIG (126 kyr BP) and the PI of $+7$ to $+11^\circ\text{C}$,
9 with $+8^\circ\text{C}$ being considered the most likely estimate. Antarctic ice cores indicate positive temperature
10 anomalies of up to $+3.5^\circ\text{C}$ (Capron et al., 2014), suggesting stronger warming than the simulated TS.
11 However, a reduction in GIS reduces the model-data disagreement. Moreover, our study does not
12 account for possible changes in the Antarctic ice sheet topography and its potential impacts (Sutter et
13 al., 2016 and references therein).

14 We go one step further and perform an additional model–data comparison with global coverage
15 (Turney and Jones, 2010). This proxy compilation is included in another model–data comparison study
16 for the LIG (Lunt et al., 2013), using a multi-model approach including the LIG-GHG. None of the
17 model simulations used in their study consider a reduction of the GIS elevation or albedo. Lunt et al.
18 (2013) find as well that the models fail to capture the magnitude of the temperature change suggested
19 by the proxy data. In their study, none of the simulations manage to capture a strong high latitude
20 annual mean warming indicated by the terrestrial proxy data. In fact, most of the models suggest a
21 slight cooling over Europe and northern Asia and only a slight warming over Greenland, at 130 kyr BP.
22 The LIG-1300m-alb indicates a relatively higher warming, reducing the disagreement between model
23 and data. Over Antarctica, the simulated and reconstructed temperature anomalies indicate a warming
24 of similar magnitude, in contrast to the simulations performed by Lunt et al. (2013), where most of the
25 models indicate a slight cooling. These results imply that a reduced GIS during the LIG improves the
26 model-data comparison. The RMSD values support this assumption (Table S2), although differences
27 between the considered cases (i.e. with or without a reduction in GIS) are relatively small – in the
28 calculation of the RMSD, all the proxy records by Turney and Jones (2010) are considered, including a
29 large number of records in the low latitudes where a change in GIS has no influence.

30 In all considered simulations, the model does not capture the magnitude of the SST anomalies
31 derived from marine records. Such underestimation of temperature changes derived from proxy data by

1 the models is also found in model-data comparison studies for the Holocene (Masson-Delmotte et al.,
2 2006; Brewer et al., 2007; Sundqvist et al., 2010; Zhang et al., 2010; O'ishi and Abe-Ouchi, 2011;
3 Braconnot et al., 2012; Lohmann et al., 2013; Bakker et al., 2014). Lohmann et al. (2013) show that the
4 simulated SST trends systematically underestimate the marine proxy-based temperature trends, and
5 suggest that such discrepancies can be caused either by too simplistic interpretations of the proxy data
6 (including dating uncertainties and seasonal biases) or by underestimated long-term feedbacks in
7 climate models, a feature which is probably also valid for the LIG. ~~Such long-term feedbacks missing
8 in our model is for example the soil which has been recently implemented in COSMOS (Stärz et al.,
9 2016). A coupled ice sheet model is already implemented in the COSMOS~~This also calls to perform
10 LIG simulations in Earth system models that account for feedbacks not accounted for in our
11 simulations, such as those associated with interactive soils (Stärz et al., 2016) and interactive ice sheet
12 model components (Barbi et al., 2014; Gierz et al., 2015), but is a relatively new tool. For instance, GIS
13 is expected to thicken at the start of an interglacial period due to enhanced accumulation associated
14 with deglacial warming (see also NEEM Community members, 2013). We did not consider this in our
15 simulations, although potential effects of the ice sheets during the LIG exist (e.g. Sutter et al., 2015).

16 As shown above, the TS in low to middle latitudes experience mostly no change in our simulation, in
17 contrast to the proxy-based SST anomalies that indicate strong positive or negative temperature
18 changes. Our results partly contradict results from another early LIG (130 kyr BP) model simulation
19 (Otto-Bliesner et al., 2013). Their Community Climate System Model 3 (CCSM3) simulates mostly a
20 cooling in the ocean, with the exception of the North Atlantic Ocean south of Greenland, where the
21 anomalies have the same sign as proxy-based SSTs by Turney and Jones (2010). The terrestrial records
22 located in the high latitudes indicate however a better agreement with the LIG-1300m-alb. Even when
23 considering mid-LIG (125 kyr BP) in both studies (see Figs. S11 for our study), the terrestrial data can
24 be better reconciled with the simulation in which GIS elevation and albedo are reduced, especially over
25 Antarctica where Otto-Bliesner et al. (2013) find a cooling. Nevertheless, the difference between the
26 magnitude of change in model and reconstruction is still large. ~~Otto-Bliesner et al (2013) suggested that
27 this mismatch may arise from the lack of vegetation feedback. Here, the fact that we account for the
28 vegetation feedback challenges this explanation. One contributing factor to warmer temperatures in the
29 high latitudes in our study may be (as also proposed by Otto-Bliesner et al., 2013) the vegetation
30 feedback, which is included in our simulations.~~ Over Greenland, the CCSM3 model underestimates the
31 data amplitude of changes when compared to reconstructions, while our model simulations with

1 reduced GIS ~~capture an overestimation~~ have too large simulated changes when compared to the same
2 reconstructions. Otto-Bliesner et al. (2013) propose that the Greenland ice records may capture
3 temperatures associated with a reduction in GIS elevation. This suggests again that the LIG GIS was
4 lower, but possibly not as low as prescribed in our study. Otto-Bliesner et al. (2013) take into account
5 also possible seasonal biases considered by Lohmann et al. (2013), comparing the proxy data to
6 simulated JJA temperature anomalies for which they find the best fit, suggesting that the proxies record
7 boreal summer temperatures. In our study, however, we find the best overall fit for simulated annual
8 mean rather than summer TS (Figs. S11a and S12a) in all three cases: reduced GIS and albedo at 130
9 kyr BP (LIG-1300m-alb, Figs. 7a and 8b) and at 125 kyr BP (LIG-125k, Figs. S11a, c), and
10 preindustrial GIS at 130 kyr BP (LIG-ctl, Figs. 6c and S4b), with the best agreement between model
11 and data in the first case (Table S2). This could indicate that the proxies may indeed record annual
12 mean temperatures, but in a warmer climate caused by a reduced GIS (Fig. 7a). While the simulated
13 summer TS are closer to the proxies at some locations (e.g. Northern Asia and Europe, Figs. S7a, S8),
14 there are still more records that agree best with the simulated annual mean TS (Fig. 7a). Along with the
15 simulated increase in TS, there is an annual mean reduction in sea ice in the simulations with reduced
16 GIS compared to the PI (not shown).

17 Capron et al (2014) had compared their data compilation to two other climate model
18 simulations. The proxy data compilation by Capron et al. (2014) used in our study is also compared to
19 two different climate models, namely CCSM3 and HadCM3. For 130 kyr BP, a model-data mismatch is
20 found in both cases, as most of the records indicate strong negative anomalies, while the models
21 simulate strong positive anomalies (Capron et al., 2014), especially CCSM3 which was run with higher
22 GHG concentrations than HadCM3 and COSMOS. With respect to the difference between model and
23 data, COSMOS simulates TS closer to the temperatures derived from marine-based records, since it
24 indicates nearly no change rather than a strong opposite signal. One cause for this modest change in the
25 North Atlantic Ocean may be related to vegetation changes, which may lead to a cooling as suggested
26 above. The vegetation feedback counteracts the warming caused by predominantly higher GHG
27 concentrations; in the simulation with dynamic vegetation (LIG-ctl-tr), the CO₂ concentration is higher
28 with up to 15 ppmv than in the simulation with fixed preindustrial vegetation (LIG-GHG-tr). However,
29 higher temperatures are found for the simulation with lower GHG concentrations (LIG-GHG-tr).
30 Another cause may be the decrease in AMOC at the LIG with respect to PI leading to the bipolar
31 seesaw, a pattern that is also observed in the proxy data at 130 kyr BP. We note a relative cooling in

1 both LIG simulations south of Iceland and Greenland. This region is very sensitive to changes in the
2 AMOC as shown in observational and numerical studies (Knight et al., 2005; Latif et al., 2006; Dima
3 and Lohmann, 2009).

4 For 125 kyr BP, COSMOS simulates higher anomalies in the North Atlantic Ocean than at 130 kyr
5 BP, but lower than CCSM3 and HadCM3 which simulate SSTs closer to the reconstructed
6 temperatures. Note however that the definition of summer is different in our study than in the study by
7 Capron et al. (2014), as they calculate it as the average of July-August-September, while we consider
8 the warmest month.

9 **4.4 Limitations of model-data comparison**

10 One challenge in an effective LIG model-data comparison is the difficulty to determine an absolute
11 dating of LIG marine paleo-proxy records (e.g. Drysdale et al., 2009), as few techniques exist for this
12 purpose. The dating of most of the records is derived by lining up their benthic $\delta^{18}\text{O}$ signal to a dated
13 benthic $\delta^{18}\text{O}$ stack (Lisiecki and Raymo, 2005). This strategy allows a relative dating of sediment cores
14 beyond the time limit of radiocarbon dating (Fairbanks et al., 2005; Chiu et al., 2007; Reimer et al.,
15 2009; Shanahan et al., 2012; Reimer et al., 2013), but it may lead to an artificial synchronization of all
16 records and therefore dampen regional differences in climate records with respect to the LIG
17 chronozone. An alternative method for synchronizing different types of proxies is used in Govin et al.
18 (2012), by aligning proxy records to the AICC2012 ice core chronology. Their study shows that the
19 maximum temperature changes during the LIG is different between the two hemispheres, the records
20 from Southern Ocean and Antarctica showing an early maximum compared to the records from
21 northern high latitudes. This method is used by Capron et al. (2014) in their proxy data compilation,
22 [and further applied in Govin et al. \(2015\)](#), thus allowing for one less uncertainty in the model-data
23 comparison. However, using such a time-resolved temperature compilation does not improve our
24 model-data comparison, as when compared to the other proxy-based datasets that represent the
25 maximum LIG warmth.

26 Additionally, some proxy records that are considered as recording annual mean temperatures are
27 seasonally biased, depending on the type of the proxy or on the region (Leduc et al., 2010; Schneider et
28 al., 2010; Lohmann et al., 2013). Furthermore, defining the timing of the maximum warmth during the
29 LIG represents as well a challenge. Bakker and Renssen (2014) show that the calculation of the
30 maximum LIG temperature is largely model-dependent, indicating also geographical- and time-
31 dependency (retrieved values differ between the annual mean and warmest month temperature

1 anomalies). They propose that the time-dependency originates from the dependency of the time
2 evolution of orbital forcing on latitude and seasons, as well as from the thermal inertia of the oceans
3 and from different feedbacks in the climate system. Our model results indicate that the timing of
4 maximum LIG warmth is indeed regionally dependent (Fig. 9).

5 **5. Conclusions**

6 In this study, we have analyzed data from several LIG sensitivity simulations performed with an
7 AOGCM and have assessed the influence of the GIS on global climate. We have compared the
8 simulated TS changes to anomalies as recorded by LIG climate data synthesis of CAPE Last
9 Interglacial Project Members (2006), Turney and Jones (2010), and of Capron et al. (2014).

10 We have shown that the exact method by which GIS configuration is changed has a significant
11 influence on hemispheric temperature anomalies. A reduction in GIS by 1300 m and changes in albedo
12 enhance the warming caused by changes in the astronomical forcing by up to +5°C. The LIG is much
13 warmer than the PI, especially during summer in the Northern Hemisphere, and during winter in the
14 Southern Hemisphere as well as northern high latitudes. The influence of astronomical forcing is
15 dominant (relative to changes in GIS) in the global and Northern Hemisphere average of annual mean
16 and local summer TS, and in the Southern Hemisphere winter. Changes in GIS have the strongest
17 influence (relative to insolation changes) globally and in the Northern Hemisphere winter average TS,
18 and in the Southern Hemisphere summer.

19 Modification of the GIS alone leads to a warming mostly in the northern and southern high latitudes.
20 Cooling occurs locally in Barents Sea or Sea of Okhotsk (depending on the simulation). The warming
21 caused by a reduced GIS has a winter rather than a summer signal at both hemispheres.

22 The simulated TS underestimate the temperature changes indicated by the proxy reconstructions.
23 However, a reduction in GIS elevation and extent improves the agreement between model and data by
24 Turney and Jones (2010). In order to obtain the maximum LIG warmth, we perform and analyze
25 transient model scenarios. For the proxy data by CAPE Last Interglacial Project Members (2006) that
26 represent summer temperatures, changes in GIS are of minor importance for SSTs.

27 Throughout the LIG, winter in the northern high latitudes is characterized by high temporal
28 variability, while summer TS indicate a clear cooling trend. By considering transient simulations with
29 different boundary conditions (i.e. GIS elevation, albedo, insolation, GHG concentrations) we offer a
30 bandwidth of potential temperatures at each given time throughout the LIG, between 130 and 115 kyr
31 BP. We reduce the mismatch between model and data by additionally considering uncertainties in

1 absolute dating of the proxy reconstructions, and uncertainties in the timing of maximum LIG warmth
2 (calculated in our study as the simulated maximum LIG warmth between 130 and 120 kyr BP at each
3 given location). The missing exact time constrain in CAPE Last Interglacial Project Members (2006)
4 and Turney and Jones (2010) provides therefore an additional uncertainty and complicates direct
5 model-data comparisons. Future studies that provide a [bettermechanistic](#) multi-proxy interpretation and
6 a better representation of the climate [modelsfeedbacks](#) are needed in order to reduce the model-data
7 mismatch. Our sensitivity simulations represent a starting point for future studies on transient
8 integrations of the LIG climate that include also transient changes in GIS elevation and extent, and for
9 the comparison of such results to high-quality proxy data. More sensitivity studies on the effects of a
10 reduced GIS on global climate are required in order to understand the response of different models to
11 such changes, as the ability of the models to properly simulate future states of the GIS is critical.

12

13 *Acknowledgement.* This study has been funded by the Deutsche Forschungsgemeinschaft (DFG) under
14 grant agreement no. LO 895/8-1 through priority programme INTERDYNAMIK (SPP 1266) and is
15 part of the project “Evaluation of Eemian and Holocene Climate Variability: Synthesis of marine
16 archives with climate modelling”. We are very grateful to an anonymous Referee and Emilie Capron
17 for the in-depth and helpful comments. [We thank Valerie Masson-Delmotte for kindly editing our](#)
18 [manuscript. We acknowledge Ingo Sasgen for helpful discussions on the manuscript.](#) Furthermore, we
19 thank the many contributors for making the temperature proxy-data available. We thank Dan Lunt for
20 providing the formatted proxy-based dataset of Turney and Jones (2010) and Emilie Capron for
21 providing their temperature dataset.

22

23 **References**

- Alley, R. B., Andrews, J. T., Brigham-Grette, J., Clarke, G. K. C., Cuffey, K. M., Fitzpatrick, J. J., Funder, S., Marshall, S. J., Miller, G. H., Mitrovica, J. X., Muhs, D. R., Otto-Bliesner, B. L., Polyak, L., and White, J. W. C.: History of the Greenland Ice Sheet: paleoclimatic insights, *Quaternary Sci. Rev.*, 29, 1728–1756, doi:16/S0277-3791(99)00062-1, 2010.
- Bakker, P. and Renssen, H.: Last Interglacial model–data mismatch of thermal maximum temperatures partially explained, *Clim. Past*, 9, 1633–1644, doi:10.5194/cpd-10-739-2014, 2014.
- Bakker, P., Van Meerbeeck, C. J., and Renssen, H.: Sensitivity of the North Atlantic climate to Greenland Ice Sheet melting during the Last Interglacial, *Clim. Past*, 8, 995–1009, doi:10.5194/cp-8-995-2012, 2012.
- Bakker, P., Stone, E. J., Charbit, S., Gröger, M., Krebs-Kanzow, U., Ritz, S. P., Varma, V., Khon, V.,

- Lunt, D. J., Mikolajewicz, U., Prange, M., Renssen, H., Schneider, B., and Schulz, M.: Last interglacial temperature evolution – a model inter-comparison, *Clim. Past*, 9, 605–619, doi:10.5194/cp-9-605-2013, 2013.
- Bakker, P., Masson-Delmotte, V., Martrat, B., Charbit, S., Renssen, H., Gröger, M., Krebs-Kanzow, U., Lohman, G., Lunt, D. J., Pfeiffer, M., Phipps, S. J., Prange, M., Ritz, S. P., Schulz, M., Stenni, B., Stone, E. J., and Varma, V.: Temperature trends during the Present and Last Interglacial periods – a multi-model–data comparison, *Quaternary Sci. Rev.*, 99, 224–243, doi:10.1016/j.quascirev.2014.06.031, 2014.
- Barbi, D., Lohmann, G., Grosfeld, K., and Thoma, M.: Ice sheet dynamics within an Earth system model: coupling and first results on ice stability and ocean circulation, *Geosci. Model Dev.*, 7, 2003–2013, doi:10.5194/gmd-7-2003-2014, 2014.
- Bauch, H. A. and Erlenkeuser, H.: Interpreting glacial–interglacial changes in ice volume and climate from subarctic deep water foraminiferal $\delta^{18}\text{O}$, in: *Earth’s Climate and Orbital Eccentricity: The Marine Isotope Stage 11 Question*, edited by: Droxler, A. W., Poore, R. Z., and Burckle, L. H., American Geophysical Union Monograph Series, Washington DC, 87–102, doi:10.1029/137GM07, 2003.
- Berger, A. L.: Long-term variations of daily insolation and Quaternary climatic changes, *J. Atmos. Sci.*, 35, 2362–2367, doi:10.1175/1520-0469(1978)035<2362:LTVODI>2.0.CO;2, 1978.
- Berger, A. and Loutre, M. F.: Insolation values for the climate of the last 10 million years, *Quaternary Sci. Rev.*, 10, 297–317, doi:10.1016/0277-3791(91)90033-Q, 1991.
- Braconnot, P., Otto-Bliesner, B., Harrison, S., Joussaume, S., Peterchmitt, J.-Y., Abe-Ouchi, A., Crucifix, M., Driesschaert, E., Fichet, Th., Hewitt, C. D., Kageyama, M., Kitoh, A., Loutre, M.-F., Marti, O., Merkel, U., Ramstein, G., Valdes, P., Weber, L., Yu, Y., and Zhao, Y.: Results of PMIP2 coupled simulations of the Mid-Holocene and Last Glacial Maximum – Part 2: feedbacks with emphasis on the location of the ITCZ and mid- and high latitudes heat budget, *Clim. Past*, 3, 279–296, doi:10.5194/cp-3-279-2007, 2007.
- Braconnot, P., Harrison, S., Kageyama, M., Bartlein, P., Masson-Delmotte, V., Abe-Ouchi, A., Otto-Bliesner, B., and Zhao, Y.: Evaluation of climate models using palaeoclimatic data, *Nat. Clim. Change*, 2, 417–424, doi:10.1038/nclimate1456, 2012.
- Brewer, S., Guiot, J., and Torre, F.: Mid-Holocene climate change in Europe: a data-model comparison, *Clim. Past*, 3, 499–512, doi:10.5194/cp-3-499-2007, 2007.
- Brovkin, V., Raddatz, T., Reick, C. H., Claussen, M., and Gayler, V.: Global biogeophysical interactions between forest and climate, *Geophys. Res. Lett.*, 36, L07405, doi:10.1029/2009GL037543, 2009.
- CAPE-members – Anderson, P., Bennike, O., Bigelow, N., Brigham-Grette, J., Duvall, M., Edwards, M., Fréchet, B., Funder, S., Johnsen, S., Knies, J., Koerner, R., Lozhkin, A., MacDonald, G., Marshall, S., Matthiessen, J., Miller, G., Montoya, M., Muhs, D., Otto-Bliesner, B., Overpeck, J., Reeh, N., Sejrup, H. P., Turner, C., and Velichko, A.: Last Interglacial Arctic warmth confirms polar amplification of climate change, *Quaternary Sci. Rev.*, 25, 1383–1400, doi:10.1016/j.quascirev.2006.01.033, 2006.
- Capron, E., Govin, A., Stone, E. J., Masson-Delmotte, V., Mulitza, S., Otto-Bliesner, B. L.,

- Rasmussen, T. L., Sime, L. C., Waelbroeck, C., and Wolff, E. W.: Temporal and spatial structure of multi-millennial temperature changes at high latitudes during the Last Interglacial, *Quaternary Sci. Rev.*, 103, 116–133, doi:10.1016/j.quascirev.2014.08.018, 2014.
- Carlson, A. E., Stoner, J. S., Donnelly, J. P., and Hillaire-Marcel, C.: Response of the southern Greenland Ice Sheet during the last two deglaciations, *Geology*, 36, 359–362, doi:10.1130/G24519A.1, 2008.
- Chiu, T.-C., Fairbanks, R. G., Cao, L., and Mortlock, R. A.: Analysis of the atmospheric ^{14}C record spanning the past 50,000 years derived from high-precision $^{230}\text{Th}/^{234}\text{U}/^{238}\text{U}$ and $^{231}\text{Pa}/^{235}\text{U}$ and ^{14}C dates on fossil corals, *Quaternary Sci. Rev.*, 26, 18–36, doi:10.1016/j.quascirev.2006.06.015, 2007.
- Church, J. A., Clark, P. U., Cazenave, A., Gregory, J. M., Jevrejeva, S., Levermann, A., Merrifield, M. A., Milne, G. A., Nerem, R. S., Nunn, P. D., Payne, A. J., Pfeffer, W. T., Stammer, D., and Unnikrishnan, A. S.: Sea level change, in: *Climate Change 2013: The Physical Science Basis, Contribution of Working Group I to the Fifth Assessment Report of the Intergovernmental Panel on Climate Change*, edited by: Stocker, T. F., Qin, D., Plattner, G.-K., Tignor, M., Allen, S. K., Boschung, J., Nauels, A., Xia, Y., Bex, V., and Midgley, P. M., Cambridge University Press, Cambridge, UK and New York, USA, 1137–1216, 2013.
- CLIMAP Project Members: The Last Interglacial ocean, *Quaternary Res.*, 21, 123–224, 1984.
- Collins, M., Knutti, R., Arblaster, J., Dufresne, J.-L., Fichet, T., Friedlingstein, P., Gao, X., Gurowki, W. J., Johns, T., Krinner, G., Shongwe, M., Tebaldi, C., Weaver, A. J., and Wehner, M.: Long-term climate change: projections, commitments and irreversibility, in: *Climate Change 2013: The Physical Science Basis, Contribution of Working Group I to the Fifth Assessment Report of the Intergovernmental Panel on Climate Change*, edited by: Stocker, T. F., Qin, D., Plattner, G.-K., Tignor, M., Allen, S. K., Boschung, J., Nauels, A., Xia, Y., Bex, V., and Midgley, P. M., Cambridge University Press, Cambridge, UK and New York, USA, 1029–1136, 2013.
- Colville, E. J., Carlson, A. E., Beard, B. L., Hatfield, R. G., Stoner, J. S., Reyes, A. V., and Ullman, D. J.: Sr-Nd-Pb isotope evidence for ice-sheet presence on southern Greenland during the last interglacial, *Science*, 333 (6042), 620–623, doi:10.1126/science.1204673, 2011.
- Crowley, T. J. and Kim, K.-Y.: Milankovitch forcing of the Last Interglacial sea level, *Science*, 265, 1566–1568, 1994.
- Cuffey, K. M. and Marshall, S. J.: Substantial contribution to sea-level rise during the last interglacial from the Greenland ice sheet, *Nature*, 404, 591–594, doi:10.1038/35007053, 2000.
- Dima, M. and Lohmann, G.: Evidence for Two Distinct Modes of Large-Scale Ocean Circulation Changes over the Last Century. *J. Climate*, 23, 5–16, doi:10.1175/2009JCLI2867.1, 2010.
- Dowsett, H. J., Foley, K. M., Stoll, D. K., Chandler, M. A., Sohl, L. E., Bentsen, M., Otto-Bliesner, B. L., Bragg, F. J., Chan, W.-L., Contoux, C., Dolan, A. M., Haywood, A. M., Jonas, J. A., Jost, A., Kamae, Y., Lohmann, G., Lunt, D. J., Nisancioglu, K. H., Abe-Ouchi, A., Ramstein, G., Riesselman, C. R., Robinson, M. M., Rosenbloom, N. A., Salzmann, U., Stepanek, C., Strother, S. L., Ueda, H., Yan, Q., and Zhang, Z.: Sea surface temperature of the mid-

- Piacenzian ocean: a data-model comparison, *Scientific Reports*, 3, 2013, doi:10.1038/srep02013, 2013.
- Drysdale, R. N., Hellstrom, J. C., Zanchetta, G., Fallick, A. E., Sánchez-Goñi, M. F., Couchoud, I., McDonald, J., Maas, R., Lohmann, G., and Isola, I.: Evidence for obliquity forcing of glacial Termination II, *Science*, 325, 1527–1531, doi:10.1126/science.1170371, 2009.
- Dutton, A. and Lambeck, K.: Ice volume and sea level during the last interglacial, *Science*, 337, 216–219, doi:10.1126/science.1205749, 2012.
- Dutton, A., Carlson, A., Milne, G., Long, A. J., Clark, P. U., DeConto, R., Horton, B. P., Rahmstorf, S., Raymo, M. E.: Sea-level rise due to polar ice-sheet mass loss during past warm periods, *Science*, 349 (6244), doi: 10.1126/science.aaa4019, 2015.
- Eugster, W., Rouse, W., Pielke Sr., R. A., McFadden, J. P., Baldocchi, D., Kittel, D., Chapin III, T. G. F., Liston, F. S., Vidale, G. E., Vaganov, P. L., and Chambers, E. S.: Land-atmosphere energy exchange in Arctic tundra and boreal forest: available data and feedbacks to climate, *Global Change Biol.*, 6, 84–115, doi:10.1046/j.1365-2486.2000.06015.x, 2000.
- Fairbanks, R. G., Mortlock, R. A., Chiu, T.-C., Cao, L., Kaplan, A., Guilderson, T. P., Fairbanks, T. W., Bloom, A. L., Grootes, P. M., and Nadeau, M.-J.: Radiocarbon calibration curve spanning 0 to 50,000 years BP based on paired $^{230}\text{Th}/^{234}\text{U}/^{238}\text{U}$ and ^{14}C dates on pristine corals, *Quaternary Sci. Rev.*, 24, 1781–1796, doi:10.1016/j.quascirev.2005.04.007, 2005.
- Felis, T., Lohmann, G., Kuhnert, H., Lorenz, S. J., Scholz, D., Pätzold, J., Al Rousan, S. A., and Al-Moghrabi, S. M.: Increased seasonality in Middle East temperatures during the last interglacial period, *Nature*, 429, 164–168, doi:10.1038/nature02546, 2004.
- Felis, T., Giry, C., Scholz, D., Lohmann, G., Pfeiffer, M., Pätzold, J., Kölling, M., and Scheffers, S. R.: Tropical Atlantic temperature seasonality at the end of the last interglacial, *Nature Comm.*, 6, 6159, doi:10.1038/ncomms7159, 2015.
- Fitzjarrald, D. R. and Moore, K. E.: Turbulent transport over tundra, *J. Geophys. Res.-Atmos.*, 97, 16717–16729, doi:10.1029/91JD01030, 1992.
- Flato, G., Marotzke, J., Abiodun, B., Braconnot, P., Chou, S. C., Collins, W., Cox, P., Driouech, F., Emori, S., Eyring, V., Forest, C., Gleckler, P., Guilyardi, E., Jakob, C., Kattsov, V., Reason, C., and Rummukainen, M.: Evaluation of climate models, in: *Climate Change 2013: The Physical Science Basis, Contribution of Working Group I to the Fifth Assessment Report of the Intergovernmental Panel on Climate Change*, edited by: Stocker, T. F., Qin, D., Plattner, G.-K., Tignor, M., Allen, S. K., Boschung, J., Nauels, A., Xia, Y., Bex, V., and Midgley, P. M., Cambridge University Press, Cambridge, UK and New York, USA, 741–866, 2013.
- [Fowler, C. M. R.: The Solid Earth: an introduction to global geophysics, Cambridge University Press, doi:10.1017/CBO9780511819643, 2004.](https://doi.org/10.1017/CBO9780511819643)
- Gauss, C. F. and Stewart, G. W.: *Theory of the Combination of Observations Least Subject to Error: Part One, Part Two, Supplement*, vol. 11, *Classics in Applied Mathematics*, Society for Industrial and Applied Mathematics, doi:10.1137/1.9781611971248, 1995.
- Gierz, P., Lohmann, G., and Wei, W.: Response of Atlantic Overturning to Future Warming in a coupled Atmosphere-Ocean-Ice Sheet Model, *Geophys. Res. Lett.*, 42, 6811–6818, doi:

10.1002/2015GL065276, 2015.

- Gong, X., Knorr, G., Lohmann, G., and Zhang, X.: Dependence of abrupt Atlantic meridional ocean circulation changes on climate background states, *Geophys. Res. Lett.*, 40, 3698–3704, doi:10.1002/grl.50701, 2013.
- Gong, X., Zhang, X., Lohmann, G., Wei, W., Zhang, Xu, and Pfeiffer, M.: Higher Laurentide and Greenland ice sheets strengthen the North Atlantic ocean circulation, *Clim. Dynam.*, 1–12, doi:10.1007/s00382-015-2502-8, 2015.
- Govin, A., Braconnot, P., Capron, E., Cortijo, E., Duplessy, J.-C., Jansen, E., Labeyrie, L., Landais, A., Marti, O., Michel, E., Mosquet, E., Risebrobakken, B., Swingedouw, D., and Waelbroeck, C.: Persistent influence of ice sheet melting on high northern latitude climate during the early Last Interglacial, *Clim. Past*, 8, 483–507, doi:10.5194/cp-8-483-2012, 2012.
- Govin, A., Capron, E., Tzedakis, P. C., Verheyden, S., Ghaleb, B., Hillaire-Marcel, C., St-Onge, G., Stoner, J. S., Bassinot, F., Bazin, L., Blunier, T., Combourieu Nebout, N., El Quahabi, A., Genty, D., Gersonde, R., Jimenez-Amat, P., Landais, A., Martrat, B., Masson-Delmotte, V., Parrenin, F., Seidenkrantz, M. S., Veres, D., Waelbroeck, C., and Zahn, R.: Sequence of events from the onset to the demise of the Last Interglacial: evaluating strengths and limitations of chronologies used in climatic archives, *Quaternary Sci. Rev.*, 129, 1–36, doi:10.1016/j.quascirev.2015.09.018, 2015.
- Harrison, S. P., Kutzbach, J. E., Prentice, C. E., Behling, P. J., and Sykes, M. T.: The response of Northern Hemisphere extratropical climate and vegetation to orbitally induced changes in insolation during the last interglaciation, *Quaternary Res.*, 43, 174–184, doi:10.1006/qres.1995.1018, 1995.
- Herold, M. and Lohmann, G.: Eemian tropical and subtropical African moisture transport: an isotope modelling study, *Clim. Dynam.*, 33, 1075–1088, doi:10.1007/s00382-008-0515-2, 2009.
- Hibler, W.: Dynamic thermodynamic sea ice model, *J. Phys. Oceanogr.*, 9, 815–846, 1979.
- Jansen, E., Overpeck, J., Briffa, K. R., Duplessy, J.-C., Joos, F., Masson-Delmotte, V., Olago, D., Otto-Bliesner, B., Peltier, W. R., Rahmstorf, S., Ramesh, R., Raynaud, D., Rind, D., Solomina, O., Villalba, R., and Zhang, D.: Palaeoclimate, in: *Climate Change 2007: The Physical Science Basis, Contribution of Working Group I to the Fourth Assessment Report of the Intergovernmental Panel on Climate Change*, edited by: Solomon, S., Qin, D., Manning, M., Chen, Z., Marquis, M., Averyt, K. B., Tignor, M., and Miller, H. L., Cambridge University Press, Cambridge, UK and New York, USA, 433–497, 2007.
- Jennings, R., Singarayer, J., Stone, E. J., Krebs-Kanzow, U., Khon, V., Nisancioglu, K. H., Pfeiffer, M., Zhang, X., Parker, A. G., Parton, A., Groucutt, H. S., White, T. S., Drake, N. A., and Petraglia, M. D.: The greening of Arabia: multiple opportunities for human occupation of the Arabian Peninsula during the Late Pleistocene inferred from an ensemble of climate model simulations, *Quatern. Int.*, 1–19, doi:10.1016/j.quaint.2015.01.006, 2015.
- Johnsen, S. J. and Vinther, B. M.: Greenland stable isotopes, in: *Encyclopedia of Quaternary Science*, Elsevier, 1250–1258, doi:10.1016/B0-444-52747-8/00345-8, 2007.
- Johnsen, S. J., Dahl-Jensen, D., Gundestrup, N., Steffensen, J.-P., Clausen, H. B., Miller, H.,

- Masson-Delmotte, V., Sveinbjornsdottir, A. E., and White, J.: Oxygen isotope and palaeotemperature records from six Greenland ice-core stations: Camp Century, Dye-3, GRIP, GISP2, Renland and NorthGRIP, *J. Quaternary Sci.*, 16, 299–307, doi:10.1002/jqs.622, 2001.
- Joussaume, S. and Braconnot, P.: Sensitivity of paleoclimate simulation results to season definitions, *J. Geophys. Res.*, 102, 1943–1956, doi:10.1029/96JD01989, 1997.
- Jungclauss, J. H., Keenlyside, N., Botzet, M., Haak, H., Luo, J. J., Latif, M., Marotzke, J., Mikolajewicz, U., and Roeckner, E.: Ocean circulation and tropical variability in the coupled model ECHAM5/MPI-OM, *J. Climate*, 19, 3952–3972, doi:10.1175/JCLI3827.1, 2006.
- Kaspar, F. and Cubasch, U.: Simulations of the Eemian interglacial and the subsequent glacial inception with a coupled ocean atmosphere general circulation model, in: *The Climate of Past Interglacials*, edited by: Sirocko, F., Litt, T., Claussen, M., and Sánchez-Goñi, M. F., Elsevier, *Developments in Quaternary Sciences*, 7, Chap. 33, 499–515, doi:10.1016/S1571-0866(07)80058-3, 2007.
- Kaspar, F., Kühl, N., Cubasch, U., and Litt, T.: A model–data comparison of European temperatures in the Eemian interglacial, *Geophys. Res. Lett.*, 32, L11703, doi:10.1029/2005GL022456, 2005.
- Kirtman, B., Power, S. B., Adedoyin, J. A., Boer, G. J., Bojariu, R., Camilloni, I., Doblas-Reyes, F. J., Fiore, A. M., Kimoto, M., Meehl, G. A., Prather, M., Sarr, A., Schär, C., Sutton, R., van Oldenborgh, G. J., Vecchi, G., and Wang, H. J.: Near-term climate change: projections and predictability, in: *Climate Change 2013: The Physical Science Basis. Contribution of Working Group I to the Fifth Assessment Report of the Intergovernmental Panel on Climate Change*, edited by: Stocker, T. F., Qin, D., Plattner, G.-K., Tignor, M., Allen, S. K., Boschung, J., Nauels, A., Xia, Y., Bex, V., and Midgley, P. M., Cambridge University Press, Cambridge, UK and New York, USA, 953–1028, 2013.
- Knight, R. A., Allan, R. J., Folland, C. K., Vellinga, M., and Mann, M. E. A.: A signature of persistent natural thermohaline circulation cycles in observed climate, *Geophys. Res. Lett.*, 32, L20708, doi:10.1029/2005GL024233, 2005.
- Knorr, G. and Lohmann, G.: A warming climate during the Antarctic ice sheet growth at the Middle Miocene transition, *Nat. Geosci.*, 7, 376–381, doi:10.1038/NGEO2119, 2014.
- Knorr, G., Butzin, M., Micheels, A., and Lohmann, G.: A warm Miocene climate at low atmospheric CO₂ levels, *Geophys. Res. Lett.*, 38, L20701, doi:10.1029/2011GL048873, 2011.
- Koerner, R. M.: Ice-core evidence for extensive melting of the Greenland Ice Sheet in the last interglacial, *Science*, 244, 964–968, 1989.
- Koerner, R. M. and Fisher, D. A.: Ice-core evidence for widespread Arctic glacier retreat in the last interglacial and the early Holocene, *Ann. Glaciol.*, 35, 19–24, doi:10.3189/172756402781817338, 2002.
- Kopp, R. E., Simons, F. J., Mitrovica, J. X., Maloof, A., and Oppenheimer, M.: Probabilistic assessment of sea level during the last interglacial stage, *Nature*, 462, 863–867, doi:10.1038/nature08686, 2009.
- Kopp, R. E., Simons, F. J., Mitrovica, J. X., Maloof, A., and Oppenheimer, M.: Probabilistic

- assessment of sea level variations within the last interglacial stage, *Geophys. J. Int.*, 193, 711–716, doi:10.1093/gji/ggt029, 2013.
- Kukla, G. J., Bender, M. L., de Beaulieu, J. L., Bond, G., Broecker, W. S., Cleveringa, P., Gavin, J. E., Herbert, T. D., Imbrie, J., Jouzel, J., Keigwin, L. D., Knudsen, K.-L., McManus, J. F., Merkt, J., Muhs, D. R., Müller, H., Poore, R. Z., Porter, S. C., Seret, G., Shackleton, N. J., Turner, C., Tzedakis, P. C., and Winograd, I. J.: Last interglacial climates, *Quaternary Res.*, 58, 2–13, doi:10.1006/qres.2001.2316, 2002.
- Kutzbach, J. E., Gallimore, R. G., and Guetter, P. J.: Sensitivity experiments on the effect of orbitally-caused insolation changes on the interglacial climate of high northern latitudes, *Quatern. Int.*, 10–12, 223–229, doi:10.1016/1040-6182(91)90054-R, 1991.
- [Landais, A., Masson-Delmotte, V., Capron, E., Langebroek, P. M., Bakker, P., Stone, E. J., Merz, N., Raible, C. C., Fischer, H., Orsi, A., Prié, F., Vinther, B., and Dahl-Jensen, D.: How warm was Greenland during the last interglacial period?, *Clim. Past Discuss.*, doi:10.5194/cp-2016-28, in review, 2016.](#)
- Langebroek, P. M. and Nisancioglu, K. H.: Simulating last interglacial climate with NorESM: role of insolation and greenhouse gases in the timing of peak warmth, *Clim. Past*, 10, 1305–1318, doi:10.5194/cp-10-1305-2014, 2014.
- Laskar, J., Robutel, P., Joutel, F., Gastineau, M., Correia, A. C. M., and Levrard, B.: A long-term numerical solution for the insolation quantities of the Earth, *Astron. Astrophys.*, 428, 261–285, doi:10.1051/0004-6361:20041335, 2004.
- Latif, M., Boning, C., Willebrand, J., Biastoch, A., Dengg, J., Keenlyside, N., Schweckendiek, U., and Madec, G.: Is the thermohaline circulation changing?, *J. Climate*, 19, 4631–4637, doi:10.1175/JCLI3876.1, 2006.
- Leduc, G., Schneider, R. R., Kim, J. H., and Lohmann, G.: Holocene and Eemian sea surface temperature trends as revealed by alkenone and Mg/Ca paleothermometry, *Quaternary Sci. Rev.*, 29, 989–1004, doi:10.1016/j.quascirev.2010.01.004, 2010.
- Lhomme, N., Clarke, G. K. C., and Ritz, C.: (2005): Global budget of water isotopes inferred from polar ice sheets, *Geophys. Res. Lett.*, 32, L20502, doi:10.1029/2005GL023774, 2005.
- Lisiecki, L. E. and Raymo, M. E.: A Pliocene-Pleistocene stack of 57 globally distributed benthic $\delta^{18}\text{O}$ records, *Paleoceanography*, 20, PA1003, doi:10.1029/2004PA001071, 2005.
- Lohmann, G. and Lorenz, S. J.: Orbital forcing on atmospheric dynamics during the last interglacial and glacial inception, in: *The Climate of Past Interglacials*, edited by: Sirocko, F., Claussen, M., Sánchez-Goñi, M. F., and Litt, T., Elsevier, *Developments in Quaternary Science*, 7, 527–546, 2007.
- Lohmann, G., Pfeiffer, M., Laepple, T., Leduc, G., and Kim, J.-H.: A model–data comparison of the Holocene global sea surface temperature evolution, *Clim. Past*, 9, 1807–1839, doi:10.5194/cp-9-1807-2013, 2013.
- Lorenz, S. J. and Lohmann, G.: Acceleration technique for Milankovitch type forcing in a coupled atmosphere–ocean circulation model: method and application for the Holocene, *Clim. Dynam.*, 23, 727–743, doi:10.1007/s00382-004-0469-y, 2004.

- Loulergue, L., Schilt, A., Spahni, R., Masson-Delmotte, V., Blunier, T., Lemieux, B., Barnola, J.-M., Raynaud, D., Stocker, T. F., and Chappellaz, J.: Orbital and millennial-scale features of atmospheric CH₄ over the past 800,000 years, *Nature*, 453, 383–386, doi:10.1038/nature06950, 2008.
- Loutre, M. F., Fichet, T., Goosse, H., Huybrechts, P., Goelzer, H., and Capron, E.: Factors controlling the last interglacial climate as simulated by LOVECLIM1.3, *Climate of the Past*, 10, 1541–1565, doi:10.5194/cp-10-1541-2014, 2014.
- Lüthi, D., Le Floch, M., Bereiter, B., Blunier, T., Barola, J. M., Siegenthaler, U., Raynaud, D., Jouzel, J., Fischer, H., Kawamura, K., and Stocker, T. F.: High-resolution carbon dioxide concentration record 650,00–800,000 years before present, *Nature*, 453, 379–382, doi:10.1038/nature06949, 2008.
- Lunt, D. J., Abe-Ouchi, A., Bakker, P., Berger, A., Braconnot, P., Charbit, S., Fischer, N., Herold, N., Jungclaus, J. H., Khon, V. C., Krebs-Kanzow, U., Langebroek, P. M., Lohmann, G., Nisancioglu, K. H., Otto-Bliesner, B. L., Park, W., Pfeiffer, M., Phipps, S. J., Prange, M., Rachmayani, R., Renssen, H., Rosenbloom, N., Schneider, B., Stone, E. J., Takahashi, K., Wei, W., Yin, Q., and Zhang, Z. S.: A multi-model assessment of last interglacial temperatures, *Clim. Past*, 9, 699–717, doi:10.5194/cp-9-699-2013, 2013.
- Marsland, S. J., Haak, H., Jungclaus, J. H., Latif, M., and Röske, F.: The Max-Planck-Institute global ocean/sea ice model with orthogonal curvilinear coordinates, *Ocean Model.*, 5, 91–127, doi:10.1016/S1463-5003(02)00015-X, 2003.
- Masson-Delmotte, V., Kageyama, M., Braconnot, P., Charbit, S., Krinner, G., Ritz, C., Guilyardi, E., Jouzel, J., Abe-Ouchi, A., Crucifix, M., Gladstone, R. M., Hewitt, C. D., Kitoh, A., LeGrande, A. N., Marti, O., Merkel, U., Motoi, T., Ohgaito, R., Otto-Bliesner, B., Peltier, W. R., Ross, I., Valdes, P. J., Vettoretti, G., Weber, S. L., Wolk, F., and Yu, Y.: Past and future polar amplification of climate change: climate model intercomparisons and ice-core constraints, *Clim. Dynam.*, 26, 513–529, doi:10.1007/s00382-005-0081-9, 2006.
- [Masson-Delmotte, V., Braconnot, P., Hoffmann, G., Jouzel, J., Kageyama, M., Landais, A., Lejeune, Q., Risi, C., Sime, L., Sjolte, J., Swingedouw, D., and Vinther, B.: Sensitivity of interglacial Greenland temperature and \$\delta^{18}\text{O}\$: ice core data, orbital and increased CO₂ climate simulations, *Clim. Past*, 7, 1041–1059, doi:10.5194/cp-7-1041-2011, 2011.](#)
- Masson-Delmotte, V., Schulz, M., Abe-Ouchi, A., Beer, J., Ganopolski, A., González Rouco, J. F., Jansen, E., Lambeck, K., Luterbacher, J., Naish, T., Osborn, T., Otto-Bliesner, B., Quinn, T., Ramesh, R., Rojas, M., Shao, X., and Timmermann, A.: Information from Paleoclimate archives, in: *Climate Change 2013: The Physical Science Basis, Contribution of Working Group I to the Fifth Assessment Report of the Intergovernmental Panel on Climate Change*, edited by: Stocker, T. F., Qin, D., Plattner, G.-K., Tignor, M., Allen, S. K., Boschung, J., Nauels, A., Xia, Y., Bex, V., and Midgley, P. M., Cambridge University Press, Cambridge, UK and New York, USA, 383–464, 2013.
- McKay, N. P., Overpeck, J. T., and Otto-Bliesner, B. L.: The role of ocean thermal expansion in Last Interglacial sea level rise, *Geophys. Res. Lett.*, 38, L14605, doi:10.1029/2011GL048280, 2011.

- Mearns, L. O., Hulme, M., Carter, T. R., Leemans, R., Lal, M., and Whetton, P.: Climate scenario development, in: *Climate Change 2001: The Scientific Basis, Contribution of Working Group I to the Third Assessment Report of the Intergovernmental Panel on Climate Change*, edited by: Houghton, J. T., Ding, Y., Griggs, D. J., Noguer, M., van der Linden, P. J., Dai, X., Maskell, K., and Johnson, C. A., Cambridge University Press, Cambridge, UK and New York, USA, 739–768, 2001.
- Merz, N., Born, A., Raible, C. C., Fischer, H., and Stocker, T. F.: Dependence of Eemian Greenland temperature reconstructions on the ice sheet topography, *Clim. Past*, 10, 1221–1238, doi:10.5194/cp-10-1221-2014, 2014.
- Montoya, M., von Storch, H., and Crowley, T. J.: Climate simulation for 125 kyr BP with a coupled ocean–atmosphere general circulation model, *J. Climate*, 13, 1057–1071, doi:10.1175/1520-0442(2000)013<1057:CSFKBW>2.0.CO;2, 2000.
- Mudelsee, M.: *Climate Time Series Analysis, Classical Statistical and Bootstrap Methods, Atmospheric and Oceanographic Sciences Library*, vol. 42, Springer, Dordrecht, 2010.
- NEEM community members: Eemian interglacial reconstructed from a Greenland folded ice core, *Nature*, 493, 498–494, doi:10.1038/nature11789, 2013.
- New, M., Hulme, M., and Jones, P.: Representing twentieth-century space–time climate variability, Part I: Development of a 1961–90 mean monthly terrestrial climatology, *J. Climate*, 12, 829–856, doi:10.1175/1520-0442(1999)012<0829:RTCSTC>2.0.CO;2, 1999.
- North Greenland Ice Core Project members: High-resolution record of Northern Hemisphere climate extending into the last interglacial period, *Nature*, 431, 147–151, doi:10.1038/nature02805, 2004.
- O’ishi, R. and Abe-Ouchi, A.: Polar amplification in the mid-Holocene derived from dynamical vegetation change with a GCM, *Geophys. Res. Lett.*, 38, L14702, doi:10.1029/2011GL048001, 2011.
- Otto-Bliesner, B. L., Marshall, S. J., Overpeck, J. T., Miller, G. H., Hu, A., and CAPE Last Interglacial Project members: simulating Arctic Climate Warmth and Icefield Retreat in the Last Interglaciation, *Science*, 311, 1751–1753, doi:10.1126/science.1120808, 2006.
- Otto-Bliesner, B. L., Rosenbloom, N., Stone, E. J., McKay, N. P., Lunt, D. J., Brady, E. C., and Overpeck, J. T.: How warm was the last interglacial? New model – data comparisons, *Philos. T. R. Soc. A*, 371, 1–20, doi:10.1098/rsta.2013.0097, 2013.
- Overpeck, J. T., Otto-Bliesner, B. L., Miller, G. H., Muhs, D. R., Alley, R. B., and Kiehl, J. T.: Paleoclimatic evidence for future ice-sheet instability and rapid sea-level rise, *Science*, 311, 1747–1750, doi:10.1126/science.1115159, 2006.
- Pfeiffer, M. and Lohmann, G.: The Last Interglacial as simulated by an Atmosphere-Ocean General Circulation Model: sensitivity studies on the influence of the Greenland Ice Sheet, in: *Earth System Science: bridging the Gaps between Disciplines Perspectives from a Multi-disciplinary Helmholtz Research School*, edited by: Lohmann, G., Grosfeld, K., Wolf-Gladrow, D., Unnithan, V., Notholt, J., and Wegner, A., Series: SpringerBriefs in Earth System Sciences, 57–64, Springer, Heidelberg, doi:10.1007/978-3-642-32235-8, 2013.

- Quiquet, A., Ritz, C., Punge, H. J., and Salas y Méliá, D.: Greenland ice sheet contribution to sea level rise during the last interglacial period: a modelling study driven and constrained by ice core data, *Clim. Past*, 9, 353–366, doi:10.5194/cp-9-353-2013, 2013.
- Raddatz, T. J., Reick, C. H., Knorr, W., Kattge, J., Roeckner, E., Schnur, R., Schnitzler, K. G., Wetzel, P., and Jungclaus, J.: Will the tropical land biosphere dominate the climate-carbon cycle feedback during the twenty-first century?, *Clim. Dynam.*, 29, 565–574, doi:10.1007/s00382-007-0247-8, 2007.
- Reimer, P. J., Baillie, M. G. L., Bard, E., Bayliss, A., Beck, J. W., Blackwell, P. G., Bronk Ramsey, C., Buck, C. E., Burr, G. S., Edwards, R. L., Friedrich, M., Grootes, P. M., Guilderson, T. P., Hajdas, I., Heaton, T. J., Hogg, A. G., Hughen, K. A., Kaiser, K. F., Kromer, B., McCormac, F. G., Manning, S. W., Reimer, R. W., Richards, D. A., Southon, J. R., Talamo, S., Turney, C. S. M., van der Plicht, J., and Weyhenmeyer, C. E.: IntCal09 and Marine09 radiocarbon age calibration curves, 0–50,000 years cal BP, *Radiocarbon*, 51, 1111–1150, 2009.
- Reimer, P. J., Bard, E., Bayliss, A., Beck, J. W., Blackwell, P. G., Bronk Ramsey, C., Buck, C. E., Cheng, H., Edwards, R. L., Friedrich, M., Grootes, P. M., Guilderson, T. P., Hafflidason, H., Hajdas, I., Hatté, C., Heaton, T. J., Hoffmann, D. L., Hogg, A. G., Hughen, K. A., Kaiser, K. F., Kromer, B., Manning, S. W., Niu, M., Reimer, R. W., Richards, D. A., Scott, E. M., Southon, J. R., Staff, R. A., Turney, C. S. M., and van der Plicht, J.: IntCal13 and Marine13 radiocarbon age calibration curves 0–50,000 years cal BP, *Radiocarbon*, 55, 1869–1887, doi:10.2458/azu_js_rc.55.16947, 2013.
- Renssen, H., Goosse, H., Fichefet, T., Masson-Delmotte, V., and Koç, N.: The Holocene climate evolution in the high-latitude Southern Hemisphere simulated by a coupled atmosphere-sea ice-ocean-vegetation model, *Holocene*, 15, 951–964, doi:10.1191/0959683605hl869ra, 2005.
- Robinson, A., Calov, R., and Ganopolski, A.: Greenland ice sheet model parameters constrained using simulations of the Eemian Interglacial, *Clim. Past*, 7, 381–396, doi:10.5194/cp-7-381-2011, 2011.
- Roeckner, E., Bäuml, G., Bonaventura, L., Brokopf, R., Esch, M., Giorgetta, M., Hagemann, S., Kirchner, I., Kornbluh, L., Manzini, E., Rhodin, A., Schlese, U., Schulzweida, U., and Tompkins, A.: The atmospheric general circulation model ECHAM5, Part I: Model description, Tech. Rep. 349, Max Planck Institute for Meteorology, Hamburg, Germany, 2003.
- Schneider, B., Leduc, G., and Park, W.: Disentangling seasonal signals in Holocene climate trends by satellite-model-proxy integration, *Paleoceanography*, 25, PA4217, doi:10.1029/2009PA001893, 2010.
- Semtner, A. J.: A model for the thermodynamic growth of sea ice in numerical investigations of climate, *J. Phys. Oceanogr.*, 6, 379–389, 1976.
- Shanahan, T. M., Beck, J. W., Overpeck, J. T., McKay, N. P., Pigati, J. S., Peck, J. A., Scholz, C. A., Heil Jr., C. W., and King, J.: Late Quaternary sedimentological and climate changes at Lake Bosumtwi Ghana: new constraints from laminae analysis and radiocarbon age modeling, *Palaeogeogr. Palaeoclimatol.*, 361–362, 49–60, doi:10.1016/j.palaeo.2012.08.001, 2012.
- Smith, T. M. and Reynolds, R. W.: A high-resolution global sea surface temperature climatology for

- the 1961–90 base period, *J. Climate*, 11, 3320–3323, doi:10.1175/1520-0442(1998)011<3320:AHRGSS>2.0.CO;2, 1998.
- Spahni, R., Chappellaz, J., Stocker, T. F., Loulergue, L., Hausammann, G., Kawamura, K., Flückiger, J., Schwander, J., Raynaud, D., Masson-Delmotte, V., and Jouzel, J.: Atmospheric methane and nitrous oxide of the late Pleistocene from Antarctic ice cores, *Science*, 310, 1317–1321, doi:10.1126/science.1120132, 2005.
- Stärz, M., Lohmann, G., and Knorr, G.: The effect of a dynamic soil scheme on the climate of the mid-Holocene and the Last Glacial Maximum, *Clim. Past*, 12, 151–170, doi:10.5194/cp-12-151-2016, 2016.
- Stepanek, C. and Lohmann, G.: Modelling mid-Pliocene climate with COSMOS, *Geosci. Model Dev.*, 5, 1221–1243, doi:10.5194/gmd-5-1221-2012, 2012.
- Stirling, C. H., Esat, T. M., Lambeck, K., and McCulloch, M. T.: Timing and duration of the last interglacial: evidence for a restricted interval of widespread coral reef growth, *Earth Planet. Sc. Lett.*, 160, 745–762, doi:10.1016/S0012-821X(98)00125-3, 1998.
- Stone, E. J., Lunt, D. J., Annan, J. D., and Hargreaves, J. C.: Quantification of the Greenland ice sheet contribution to Last Interglacial sea level rise, *Clim. Past*, 9, 621–639, doi:10.5194/cp-9-621-2013, 2013.
- [Stone, E. J., Capron, E., Lunt, D. J., Payne, A. J., Singarayer, J. S., Valdes, P. J., and Wolff, E. W.: Impact of melt water on high latitude early Last Interglacial climate, *Clim. Past Discuss.*, doi:10.5194/cp-2016-11, in review, 2016.](#)
- Sundqvist, H. S., Zhang, Q., Moberg, A., Holmgren, K., Körnich, H., Nilsson, J., and Brattström, G.: Climate change between the mid and late Holocene in northern high latitudes – Part 1: Survey of temperature and precipitation proxy data, *Clim. Past*, 6, 591–608, doi:10.5194/cp-6-591-2010, 2010.
- Sutter, J., Gierz, P., Grosfeld, K., Thoma, M., and Lohmann, G.: Ocean temperature thresholds for Last Interglacial West Antarctic Ice Sheet collapse, *Geophys. Res. Lett.*, doi:10.1002/2016GL067818, 2016, (in press).
- Tarasov, L. and W. R. Peltier: Greenland glacial history, borehole constraints, and Eemian extent, *J. Geophys. Res.*, 108(B3), 2143, doi:10.1029/2001JB001731, 2003.
- Turney, C. S. M. and Jones, R. T.: Does the Agulhas current amplify global temperatures during super-interglacials?, *J. Quaternary Sci.*, 25, 839–843, doi:10.1002/Jqs.1423, 2010.
- Valcke, S.: The OASIS3 coupler: a European climate modelling community software, *Geosci. Model Dev.*, 6, 373–388, doi:10.5194/gmd-6-373-2013, 2013.
- Valcke, S., Caubel, A., Declat, D., and Terray, L.: OASIS Ocean Atmosphere Sea Ice Soil users guide, Tech. Rep. TR/CMGC/03-69, CERFACS, Toulouse, France, 2003.
- van de Berg, W. J., van den Broeke, M., Ettema, J., van Meijgaard, E., and Kaspar, F.: Significant contribution of insolation to Eemian melting of the Greenland ice sheet, *Nat. Geosci.*, 4, 679–683, doi:10.1038/ngeo1245, 2011.
- Veeh, H. H.: $\text{Th}^{230}/\text{U}^{238}$ and $\text{U}^{234}/\text{U}^{238}$ ages of Pleistocene high sea level stand, *J. Geophys. Res.*, 71,

3379–3386, 1966.

- von Storch, H. and Zwiers, F. W.: *Statistical Analysis in Climate Research*, Cambridge University Press, New York, 1999.
- Wei, W. and Lohmann, G.: Simulated Atlantic Multidecadal Oscillation during the Holocene, *J. Climate*, 25, 6989–7002, doi:10.1175/JCLI-D-11-00667.1, 2012.
- Wei, W., Lohmann, G., and Dima, M.: Distinct modes of internal variability in the global meridional overturning circulation associated with the SH westerly winds, *J. Phys. Oceanogr.*, 42, 785–801, doi:10.1175/JPO-D-11-038.1, 2012.
- Willerslev, E., Cappellini, E., Boomsma, W., Nielsen, R., Hebsgaard, M. B., Brand, T. B., Hofreiter, M., Bunce, M., Poinar, H. N., Dahl-Jensen, D., Johnsen, S., Steffensen, J. P., Bennike, O., Schwenninger, J.-L., Nathan, R., Armitage, S., de Hoog, C.-J., Alfimov, V., Christl, M., Beer, J., Muscheler, R., Barker, J., Sharp, M., Penkman, K. E. H., Haile, J., Taberlet, P., Gilbert, M. T. P., Casoli, A., Campani, E., and Collins, M. J.: Ancient bio-molecules from deep ice cores reveal a forested southern Greenland, *Science*, 317, 111–114, doi:10.1126/science.1141758, 2007.
- Yin, Q. Z. and Berger, A.: Insolation and CO₂ contribution to the interglacial climate before and after the Mid-Brunhes Event, *Nat. Geosci.*, 3, 243–246, doi:10.1038/ngeo771, 2010.
- Zhang, Q., Sundqvist, H. S., Moberg, A., Körnich, H., Nilsson, J., and Holmgren, K.: Climate change between the mid and late Holocene in northern high latitudes – Part 2: Model-data comparisons, *Clim. Past*, 6, 609–626, doi:10.5194/cp-6-609-2010, 2010.
- Zhang, X., Lohmann, G., Knorr, G., and Xu, X.: Different ocean states and transient characteristics in Last Glacial Maximum simulations and implications for deglaciation, *Clim. Past*, 9, 2319–2333, doi:10.5194/cp-9-2319-2013, 2013.
- Zhang, X., Lohmann, G., Knorr, G., and Purcell, C.: Control of rapid glacial climate shifts by variations in intermediate ice-sheet volume, *Nature*, 512, 290–294, doi:10.1038/nature13592, 2014.

1 **Table and Figure captions**

2

3 **Table 1.** Overview of model configuration and climate forcings. PI = preindustrial, Veg. = vegetation;
4 dyn. = dynamic; e = eccentricity; ϵ = obliquity; ω = length of perihelion. The Greenland Ice Sheet
5 (GIS) configurations are displayed in Fig. 1. * Simulations presented in the supplementary material.

6

7 **Table 2.** Atlantic Meridional Overturning Circulation (AMOC) and absolute values of surface
8 temperature (TS) for global, Northern Hemisphere (NH), and Southern Hemisphere (SH) coverage,
9 calculated for annual mean, local summer mean (warmest month), and local winter mean (coldest
10 month).

11

12 **Figure 1.** Greenland Ice Sheet (GIS) elevation and land ice cover prescribed in our model simulations:
13 **(a)** preindustrial GIS and land ice mask, **(b)** $\times 0.5$ GIS and preindustrial land ice mask, **(c)** -1300 m GIS
14 and preindustrial land ice mask, **(d)** -1300 m and adjusted land ice mask. In **(a)**, the preindustrial
15 elevation and land ice mask are unchanged. In **(b)**, the preindustrial elevation over the GIS area is
16 multiplied by 0.5; the land ice mask is unchanged. In **(c)**, for each grid point over the GIS, 1300 m are
17 subtracted from preindustrial elevation; the land ice mask is unchanged. In **(d)**, for each grid point over
18 the GIS, 1300 m are subtracted from preindustrial elevation; at grid locations where the elevation is
19 lower than 1300 m, land ice is removed and albedo is adjusted accordingly.

20

21 **Figure 2.** Effect of **(a–c)** Greenland Ice Sheet elevation and **(c, d)** albedo in the 130 kyr BP
22 simulations. Annual mean surface temperature (TS) anomalies for: **(a)** LIG- $\times 0.5$ minus LIG-ctl, **(b)**
23 LIG-1300m minus LIG-ctl, **(c)** LIG-1300m-alb minus LIG-ctl, and **(d)** LIG-1300m-alb minus LIG-
24 1300m. Hatched areas mark statistically insignificant TS anomalies.

25

26 **Figure 3.** Effect of Greenland Ice Sheet elevation and albedo on surface temperature in the 130 kyr BP
27 simulation (LIG-1300m-alb). Same as Fig. 2c but for: **(a)** local winter mean (coldest month) and **(b)**
28 local summer mean (warmest month). Violet dashed lines represent the LIG-1300m-alb 50 %-
29 compactness sea ice isoline, violet continuous lines represent the LIG-1300m-alb sea ice edge. Green
30 dashed lines represent the LIG-ctl 50 %-compactness sea ice isoline, green continuous lines represent
31 the LIG-ctl sea ice edge.

1

2 **Figure 4.** Effect of Greenland Ice Sheet elevation, insolation, and albedo at 130 kyr BP relative to
3 preindustrial (PI). Surface temperature (TS) anomalies between LIG-1300m-alb-CH₄ and PI for: **(a)**
4 annual mean, **(b)** local winter mean (coldest month), and **(c)** local summer mean (warmest month).
5 Violet dashed lines represent the LIG 50 %-compactness sea ice isoline, violet continuous lines
6 represent the LIG sea ice edge. Green dashed lines represent the PI 50 %-compactness sea ice isoline,
7 green continuous lines represent the PI sea ice edge. Hatched areas mark statistically insignificant TS
8 anomalies.

9

10 **Figure 5.** Simulated surface temperature evolution for the Last Interglacial (LIG-) and the Holocene
11 (8–0 kyr BP, HOL-tr) in northern high latitudes (60–90°N) calculated as running average with a
12 window length of 21 model years representing 210 calendar years for: **(a)** annual mean, **(b)** local winter
13 mean (coldest month), and **(c)** local summer mean (warmest month). The lower *x* scale represents the
14 LIG time scale, the upper *x* scale indicates the Holocene time scale. The upper *x* scale is matched to the
15 time scale between 128 and 120 kyr BP, assuming that Termination I and Termination II are similar
16 with respect to obliquity (Drysdale et al., 2009).

17

18 **Figure 6.** Effect of **(a, b)** Greenland Ice Sheet elevation, insolation, albedo, and atmospheric methane
19 concentration and **(c, d)** insolation and atmospheric methane concentration for the Last Interglacial
20 (LIG) relative to preindustrial (PI). Model-data comparison of mean local summer temperature
21 anomalies. The shading represents the simulated surface temperature (TS) anomalies at **(a, c)** 130 kyr
22 BP derived from **(a)** LIG- 1300 m-alb and **(c)** LIG-ctl, and **(b, d)** summer maximum LIG warmth
23 (warmest 100 warmest months between 130 and 120 kyr BP) derived from **(b)** LIG-1300m-alb-tr and
24 **(d)** LIG-ctl-tr, relative to PI. Hatched areas in **(a, c)** mark statistically insignificant TS anomalies. The
25 squares and circles show marine and terrestrial proxy-based maximum LIG summer temperature
26 anomalies relative to PI derived by CAPE Last Interglacial Project Members (2006). The colors inside
27 the squares and circles represent the proxy-based temperature anomalies derived from the intervals
28 provided by CAPE Last Interglacial Project Members (2006), that agree best with the simulated TS
29 anomalies at the location of the proxies.

30

31 **Figure 7.** Effect of **(a, b)** Greenland Ice Sheet elevation, insolation, albedo, and atmospheric methane

1 concentration and **(c, d)** insolation and atmospheric methane concentration for the Last Interglacial
2 (LIG) relative to preindustrial (PI). Model-data comparison of mean annual temperature anomalies. The
3 shading represents the simulated surface temperature (TS) anomalies at **(a, c)** 130 kyr BP derived from
4 **(a)** LIG-1300m-alb and **(c)** LIG-ctl, and **(b, d)** maximum LIG warmth (warmest 100 model years
5 between 130 and 120 kyr BP) derived from **(b)** LIG-1300m-alb-tr and **(d)** LIG-ctl-tr, relative to PI.
6 Hatched areas in **(a, c)** mark statistically insignificant TS anomalies. The squares and circles show
7 marine and terrestrial proxy-based LIG annual mean temperature anomalies relative to present-day
8 (1961–1990) derived by Turney and Jones (2010).

9
10 **Figure 8.** Effect of Greenland Ice Sheet elevation, insolation, albedo, and atmospheric methane
11 concentration for the Last Interglacial (LIG) relative to preindustrial (PI). **(a)** Proxy-based maximum
12 LIG summer temperature anomalies relative to PI derived by CAPE Last Interglacial Project Members
13 (2006) plotted against simulated local summer surface temperature (TS) anomalies at 130 kyr BP (LIG-
14 1300m-alb) relative to PI at the location of the proxies. The horizontal bars represent the proxy-based
15 temperature intervals derived by CAPE Last Interglacial Project Members (2006). The vertical bars
16 indicate the simulated TS anomalies at the maximum and minimum LIG TS with respect to local
17 summer (i.e. the coldest and warmest 100 warmest months) derived from the time interval 130 to 120
18 kyr BP (LIG-1300m-alb-tr) relative to PI, for each given proxy record location. **(b)** Proxy-based LIG
19 annual mean temperature anomalies relative to present-day (1961–1990) derived by Turney and Jones
20 (2010), plotted against simulated annual mean TS anomalies at 130 kyr BP (LIG-1300m-alb) relative to
21 PI at the location of the proxies. The vertical bars indicate the simulated TS anomalies at the maximum
22 and minimum LIG TS with respect to annual mean (i.e the coldest and warmest 100 model years)
23 derived from the time interval 130 to 120 kyr BP (LIG-1300m-alb-tr) relative to PI, for each given
24 proxy record location. **(c)** Same as **(b)** but displaying vertical bars that represent local summer and local
25 winter mean (i.e. the warmest 100 warmest months and coldest 100 coldest months). The squares (red)
26 and circles (black) represent marine and terrestrial proxy-based temperature anomalies, respectively.
27 The solid thick lines represent the 1 : 1 line that indicates a perfect match of simulated and
28 reconstructed anomalies.

29
30 **Figure 9.** Timing of the maximum Last Interglacial warmth for: **(a)** local summer (warmest 100
31 warmest months) and **(b)** annual mean (warmest 100 model years) derived from the LIG-1300m-alb-tr,

1 between 130 and 120 kyr BP.

2

3 **Figure 10.** Effect of **(a, b)** Greenland Ice Sheet elevation, insolation, albedo, and atmospheric methane
4 concentration and **(c, d)** insolation and atmospheric methane concentration at 130 kyr BP relative to
5 preindustrial (PI). Model-data comparison of mean local summer temperature anomalies. The shading
6 represents the simulated surface temperature (TS) anomalies derived from **(a, b)** LIG-1300m-alb and
7 **(c, d)** LIG-ctl. Hatched areas mark statistically insignificant TS anomalies. The squares show marine
8 proxy-based LIG (130 kyr BP) summer temperature anomalies relative to present-day derived by
9 Capron et al (2014).

10

11 **Figure 11.** Effect of **(a–c)** Greenland Ice Sheet elevation and **(c)** albedo on sea level pressure (SLP) and
12 surface winds in 130 kyr BP simulations. The shading represents December-January-February (DJF)
13 mean SLP anomalies, superimposed by DJF mean surface wind anomalies (in ms^{-1}) for: **(a)** LIG- $\times 0.5$
14 minus LIG-ctl, **(b)** LIG-1300m minus LIG-ctl, and **(c)** LIG-1300m-alb minus LIG-ctl. The vector
15 length indicates the wind speed (in ms^{-1}).

Simulation	Time (kyr BP)	CO ₂ (ppmv)	CH ₄ (ppbv)	N ₂ O (ppbv)	Greenland Ice Sheet	Veg.	e	ε (°)	ω (°)
LIG-ctl	130	278	650	270	PI	dyn.	0.0382	24.24	49.1
LIG-×0.5	130	278	650	270	×0.5	dyn.	0.0382	24.24	49.1
LIG-1300m	130	278	650	270	-1300m	dyn.	0.0382	24.24	49.1
LIG-1300m-alb	130	278	650	270	-1300m+alb	dyn.	0.0382	24.24	49.1
LIG-1300m-alb-CH ₄	130	280	760	270	-1300m+alb	dyn.	0.0382	24.24	49.1
LIG-GHG*	130	257	512	239	PI	PI	0.0382	24.24	49.1
LIG-125k*	125	278	650	270	-1300m+alb	dyn.	0.0400	23.79	128.1
PI	0	280	760	270	PI	dyn.	0.0167	23.45	282.2
LIG-ctl-tr	130-115	278	650	270	PI	dyn.	varying	varying	varying
LIG-×0.5-tr	130-115	278	650	270	×0.5	dyn.	varying	varying	varying
LIG-1300m-alb-tr	130-115	278	650	270	-1300m+alb	dyn.	varying	varying	varying
LIG-GHG-tr	130-115	varying	varying	varying	PI	PI	varying	varying	varying
HOL-tr	8-0	278	650	270	PI	dyn.	varying	varying	varying

Table 1

Simulation	AMOC (Sv)	Annual mean TS (°C)			Winter mean TS (°C)			Summer mean TS (°C)		
		global	NH	SH	global	NH	SH	global	NH	SH
LIG-ctl	12.8	14.77	15.57	13.98	8.76	6.53	10.98	21.00	24.78	17.22
LIG- $\times 0.5$	13.3	15.13	16.03	14.22	9.19	7.12	11.25	21.25	25.09	17.41
LIG-1300m	14.8	15.07	15.95	14.18	9.14	7.05	11.22	21.17	24.96	17.39
LIG-1300m-alb	15.0	15.14	16.00	14.29	9.24	7.10	11.37	21.24	25.02	17.46
LIG-1300m-alb-CH ₄	14.4	15.32	16.34	14.29	9.40	7.49	11.31	21.43	25.35	17.50
LIG-GHG	12.8	14.65	15.50	13.80	8.69	6.56	10.82	20.82	24.64	17.00
LIG-125k	14.8	15.19	16.11	14.27	9.46	7.74	11.17	21.20	24.94	17.46
PI	16.3	14.51	15.35	13.67	8.84	7.44	10.23	20.09	22.84	17.33

Table 2

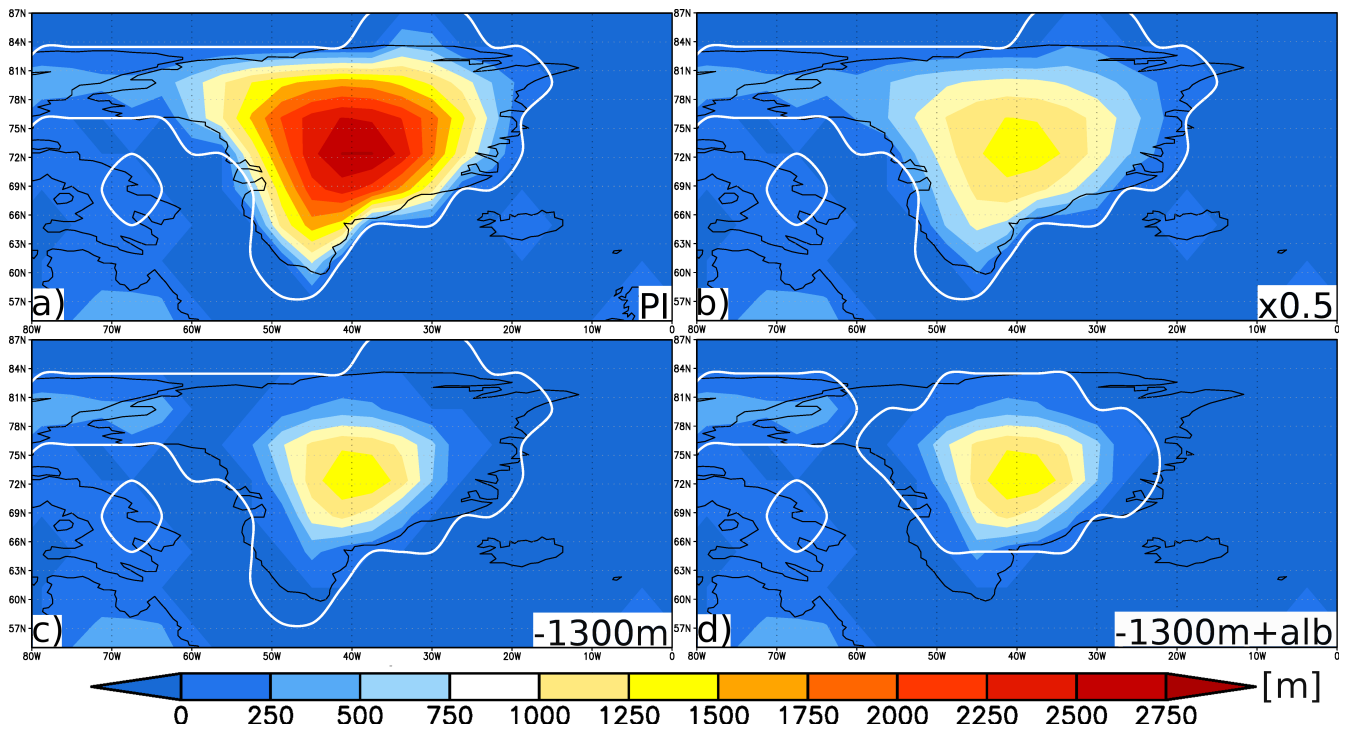


Figure 1

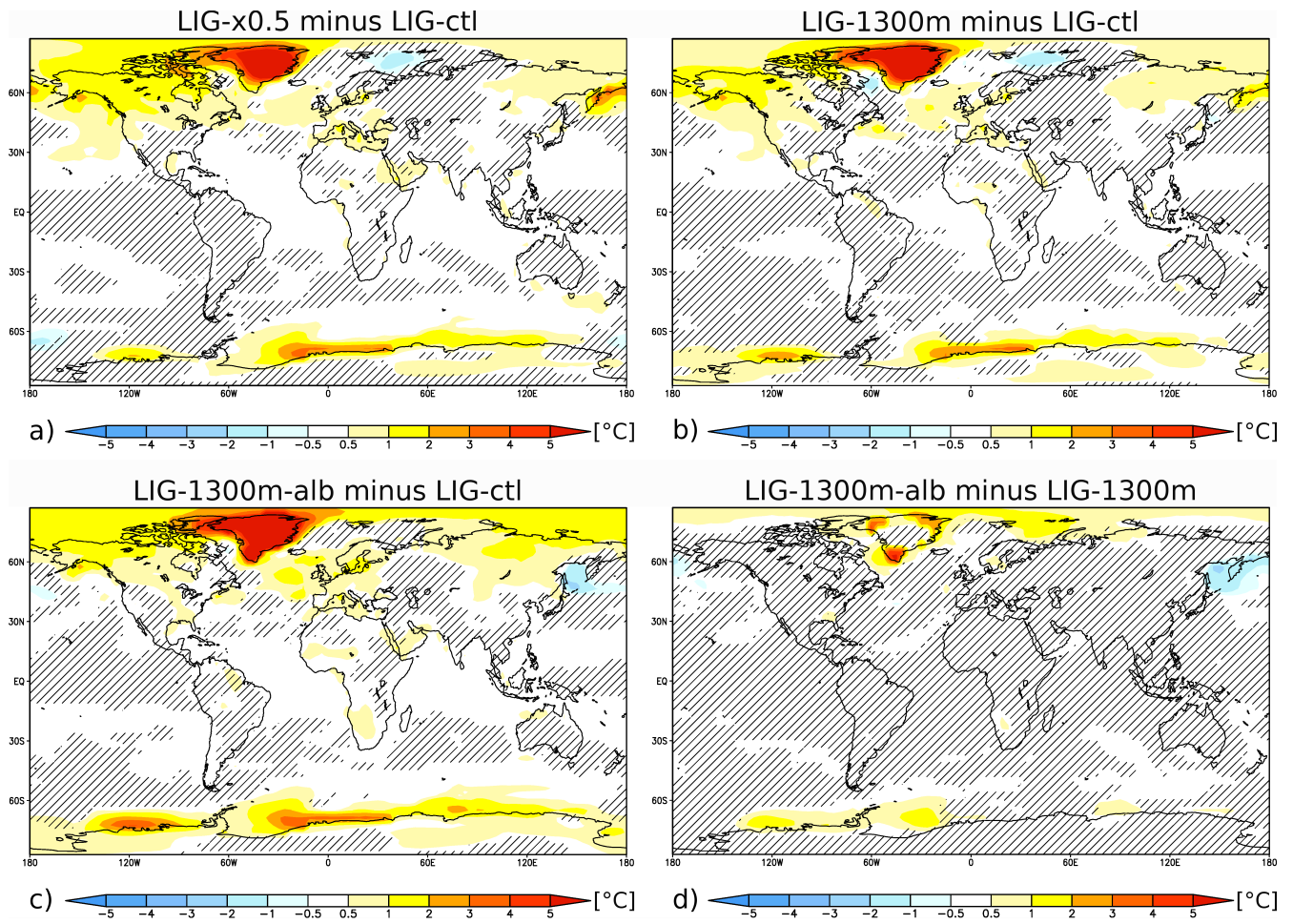
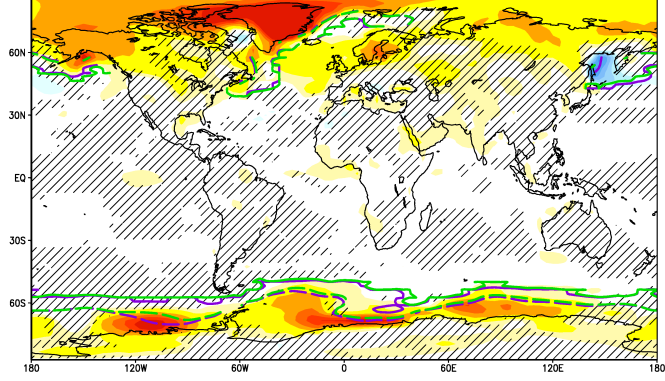


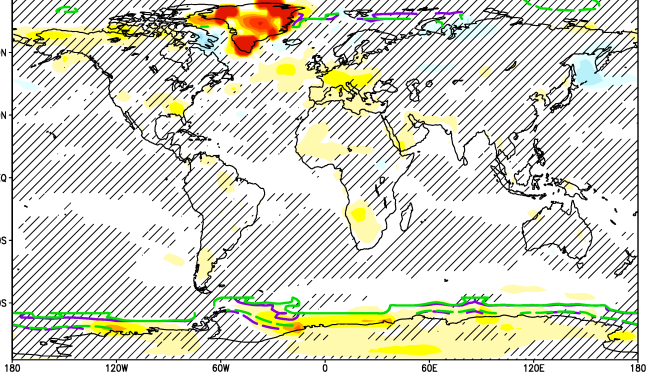
Figure 2

LIG-1300m-alb minus LIG-ctl (local winter)



a) [°C]

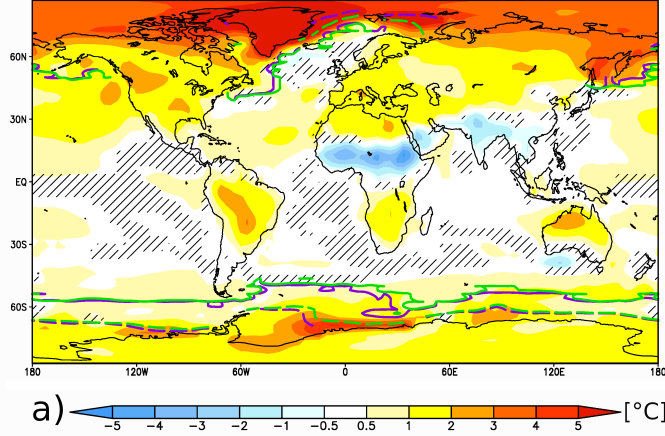
LIG-1300m-alb minus LIG-ctl (local summer)



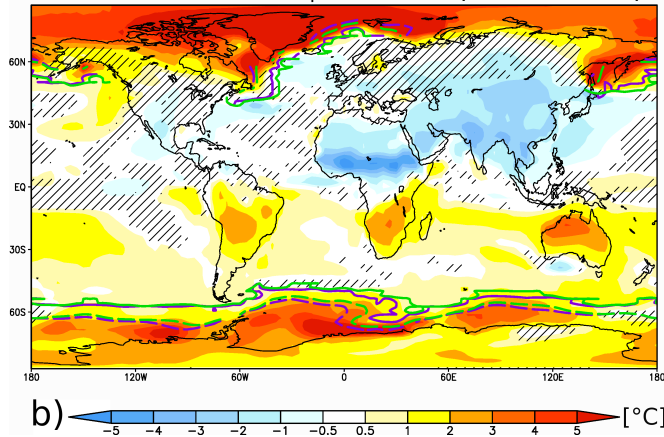
b) [°C]

Figure 3

LIG-1300m-alb-CH₄ minus PI (annual mean)



LIG-1300m-alb-CH₄ minus PI (local winter)



LIG-1300m-alb-CH₄ minus PI (local summer)

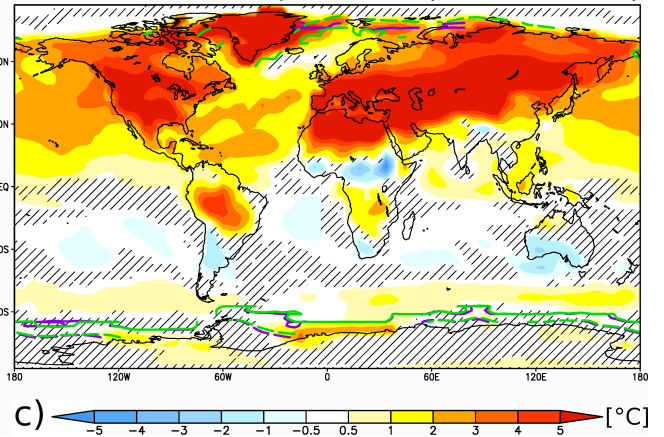


Figure 4

Northern high latitudes (60-90°N)

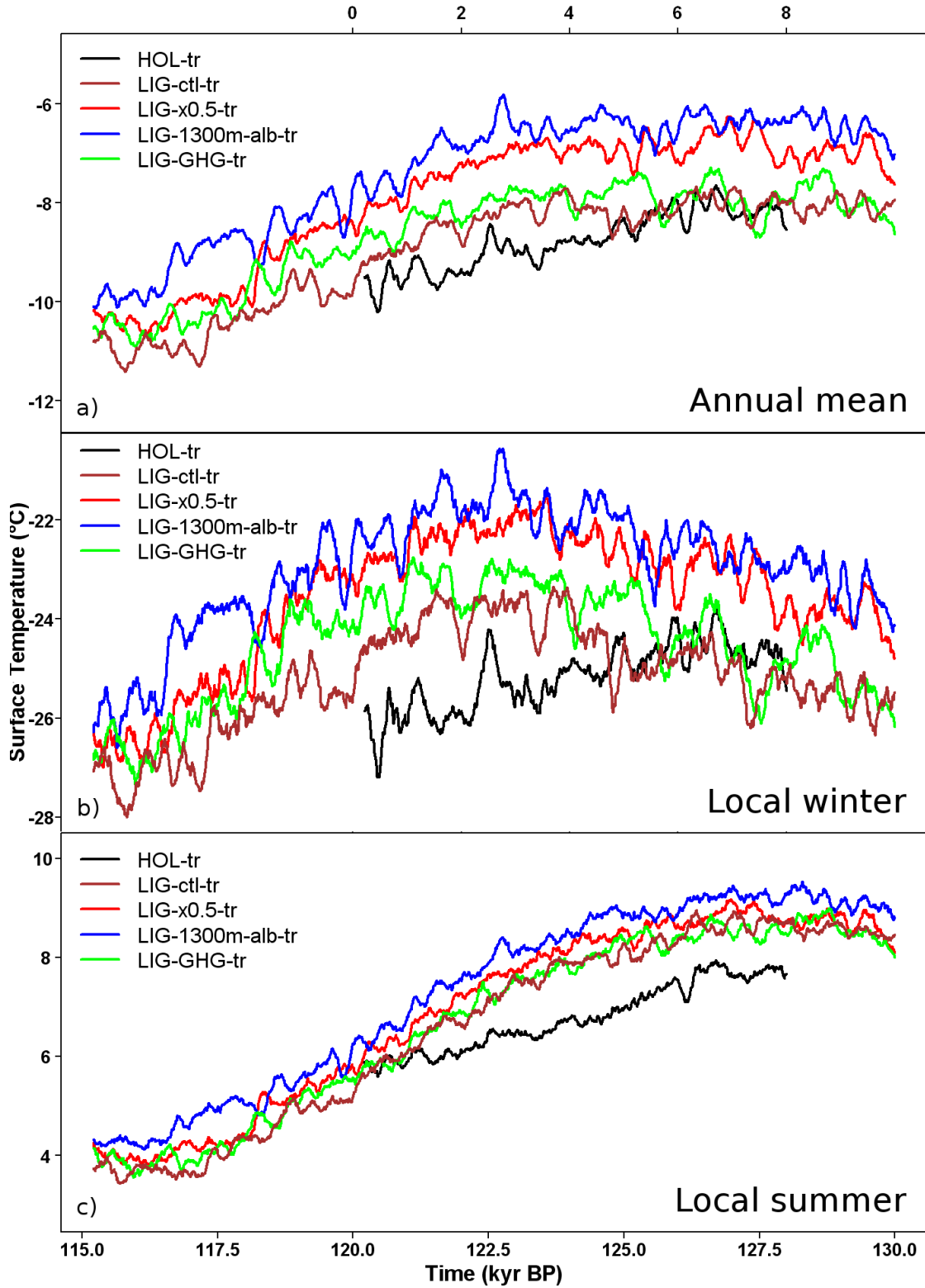
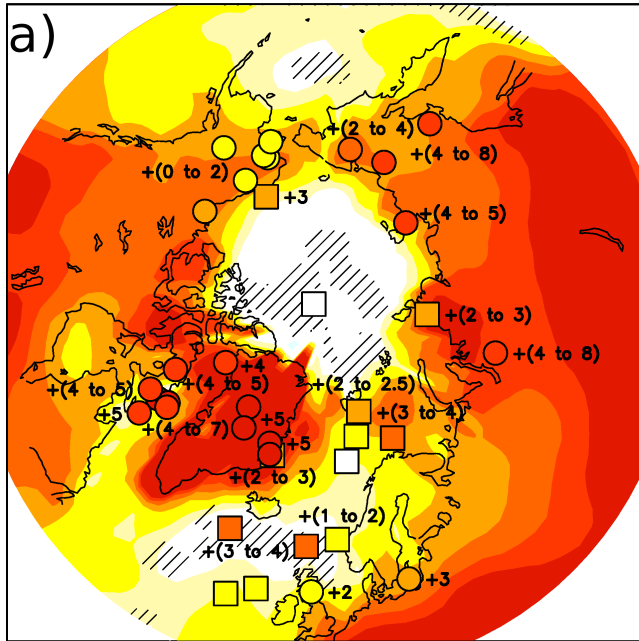


Figure 5

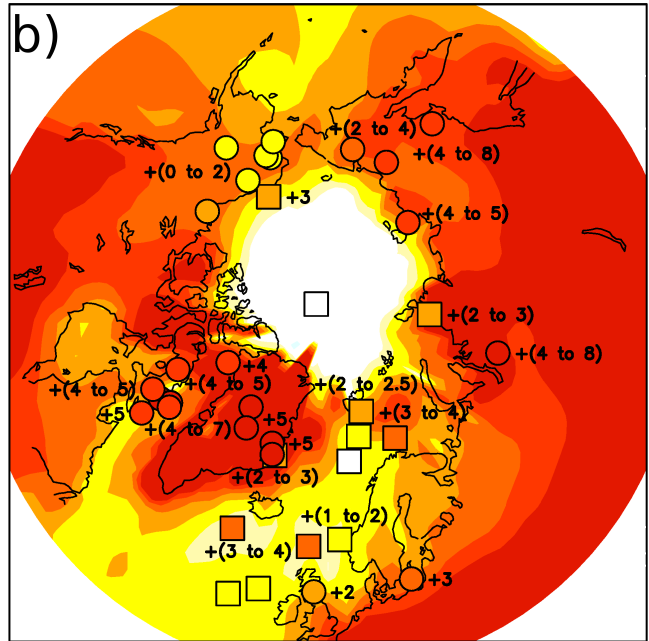
Local summer at 130 kyr BP

LIG-1300m-alb minus PI

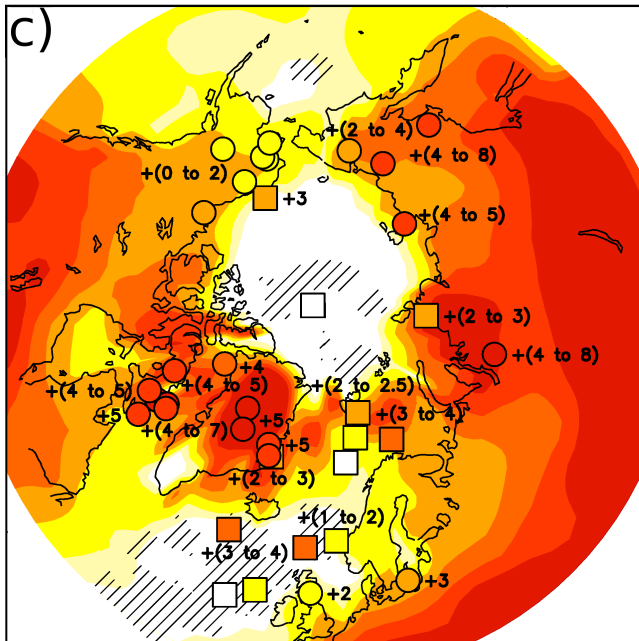


Local summer at maximum LIG warmth

LIG-1300m-alb-tr minus PI



LIG-ctl minus PI



LIG-ctl-tr minus PI

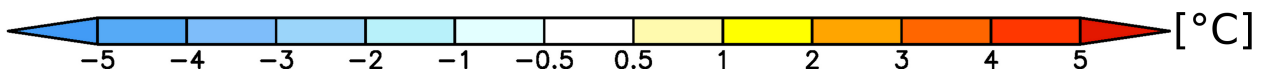
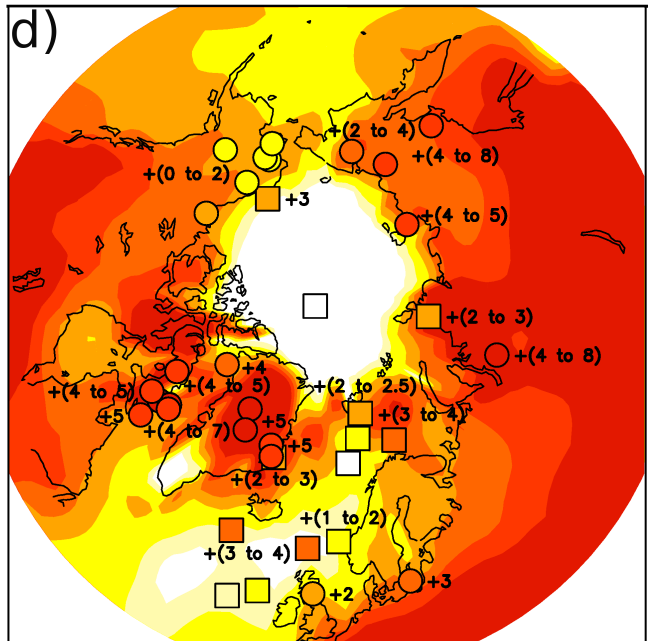
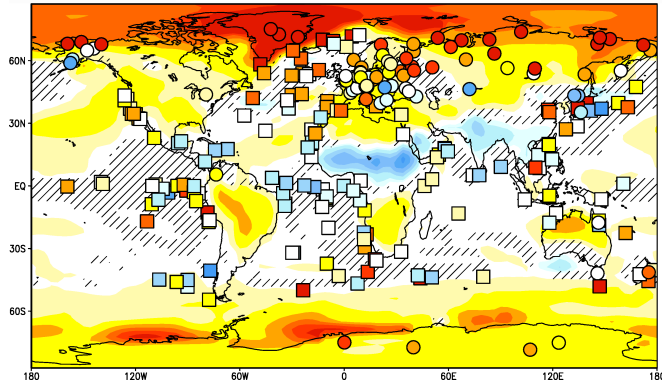


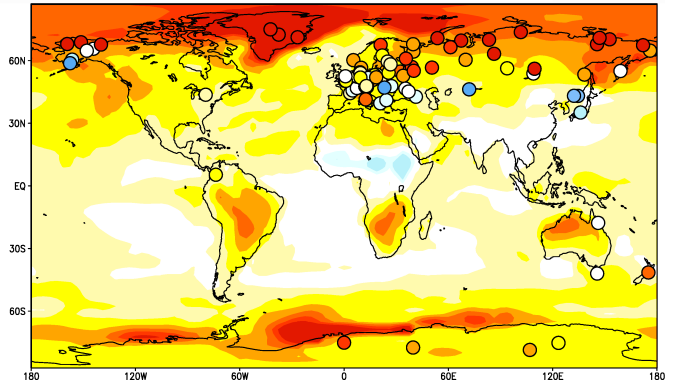
Figure 6

Annual mean at 130 kyr BP
LIG-1300m-alb minus PI



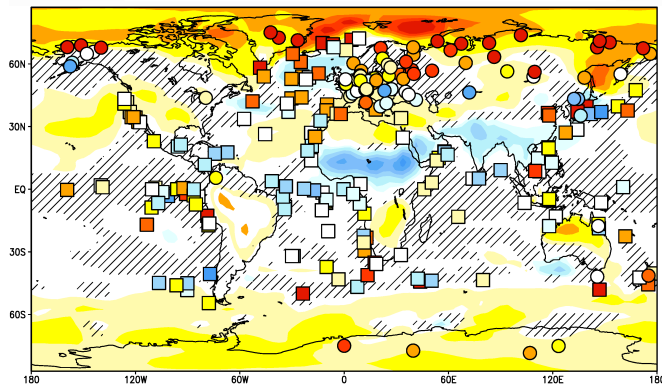
a) [°C]

Annual mean at maximum LIG warmth
LIG-1300m-alb-tr minus PI



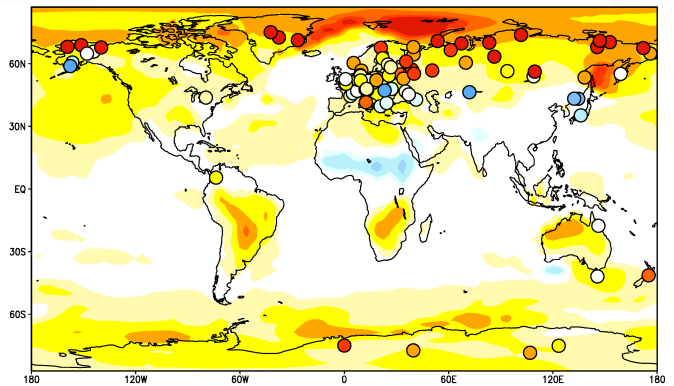
b) [°C]

LIG-ctl minus PI



c) [°C]

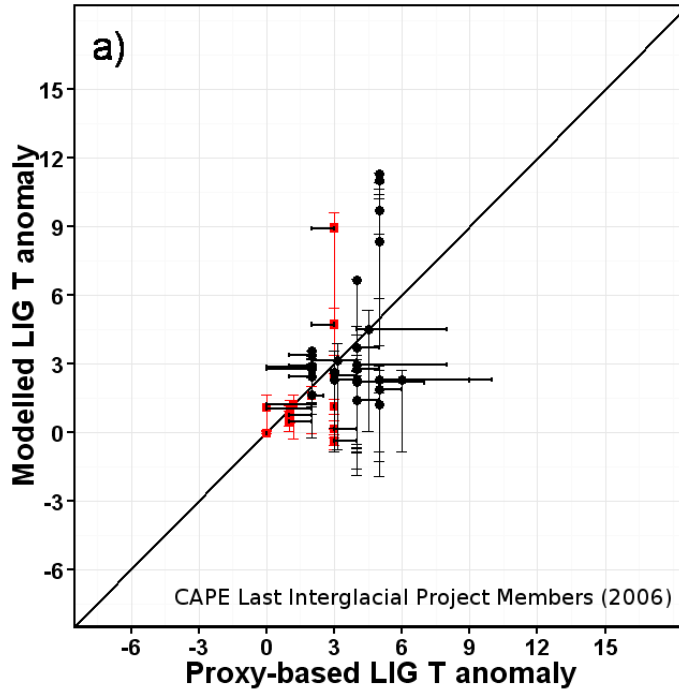
LIG-ctl-tr minus PI



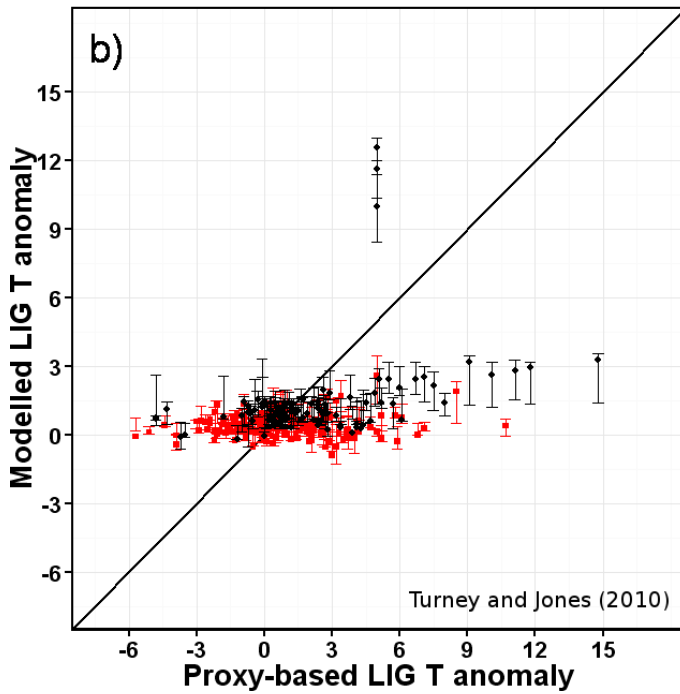
d) [°C]

Figure 7

Proxy vs. simulated local summer [°C]



Proxy vs. simulated annual mean [°C]



Proxy vs. simulated annual mean, local winter and summer [°C]

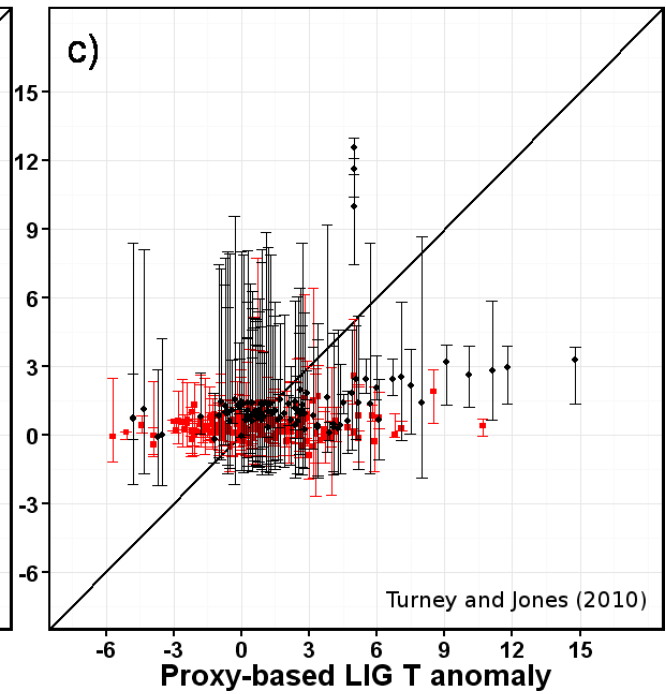


Figure 8

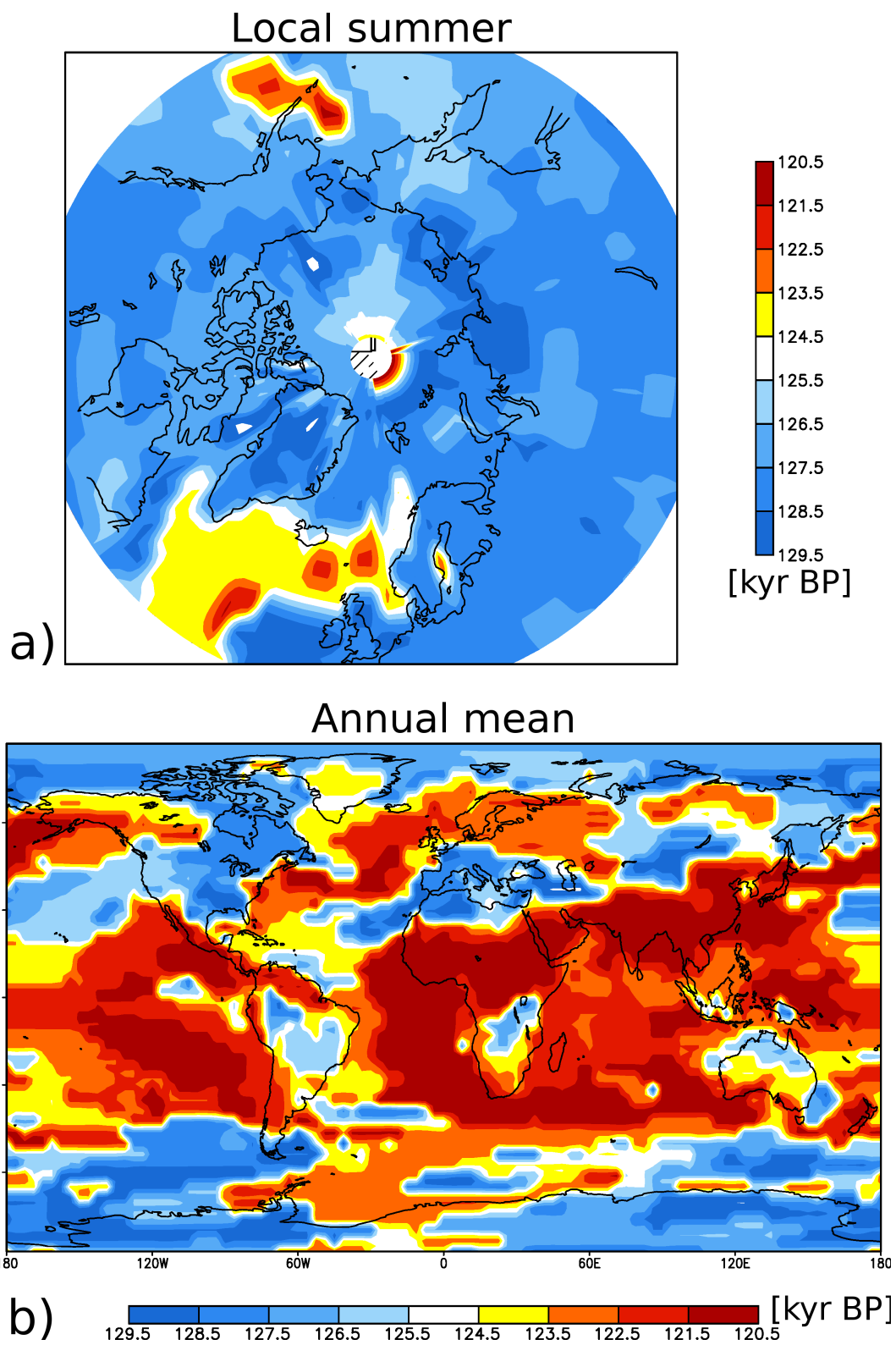
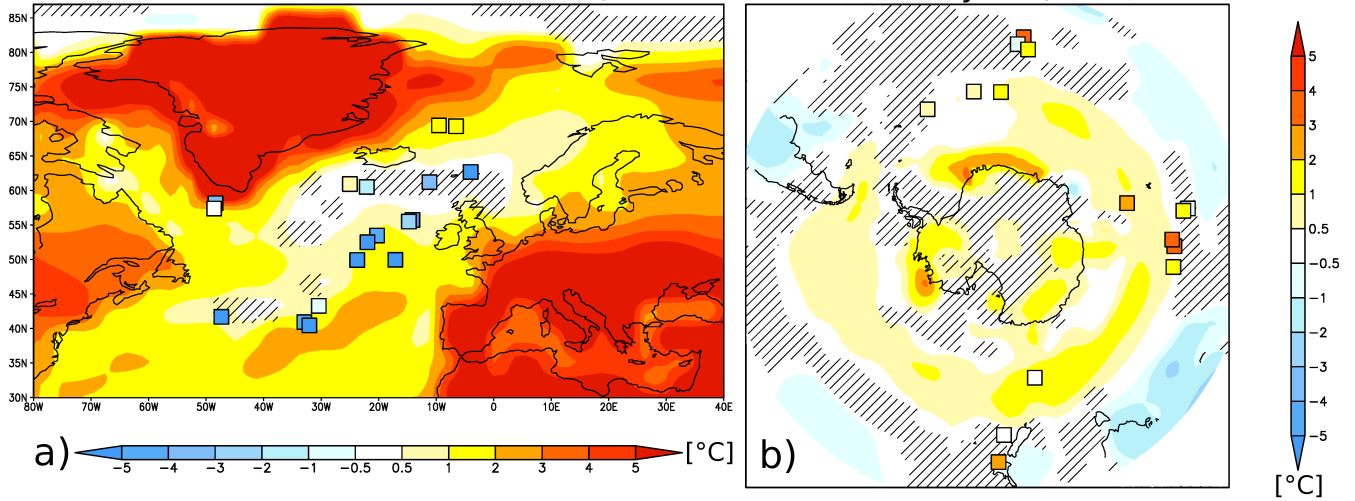


Figure 9

LIG-1300m-alb minus PI (local summer at 130 kyr BP)



LIG-ctl minus PI (local summer at 130 kyr BP)

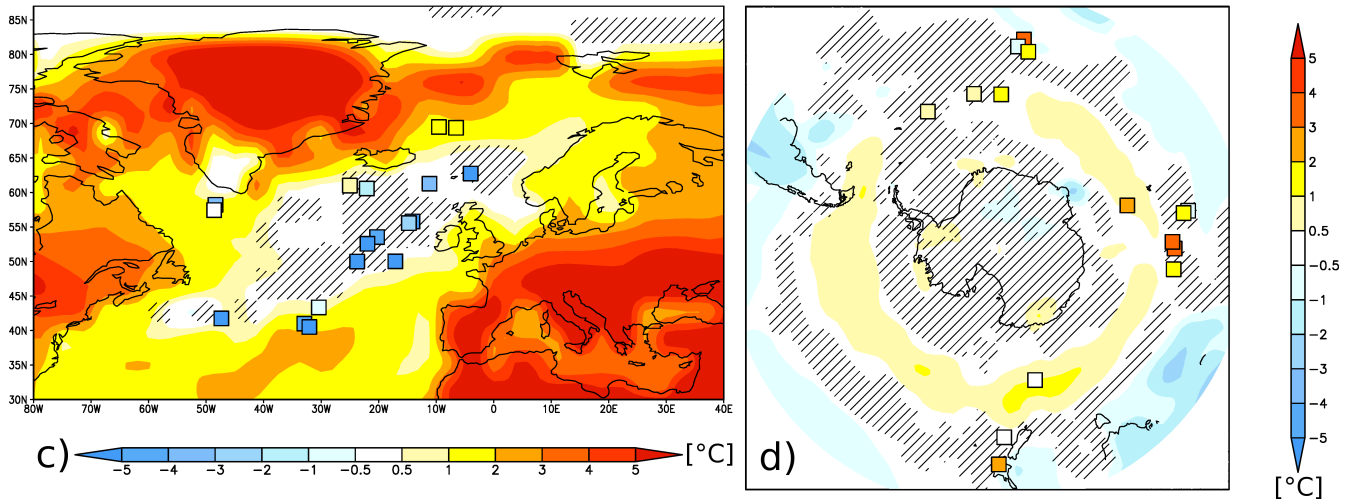


Figure 10

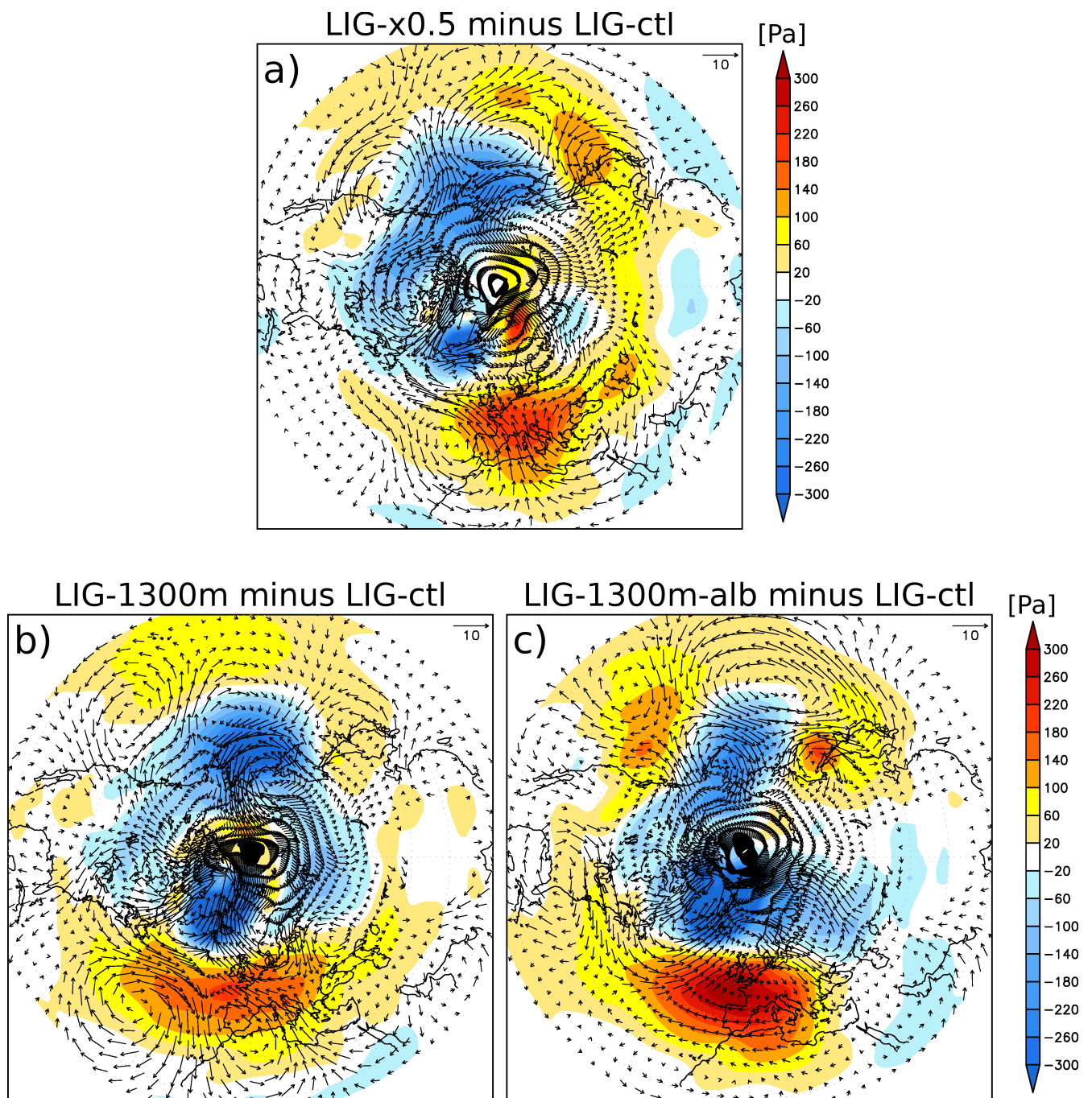


Figure 11